Ferromagnetic Behavior of $[Fe(C_5Me_5)_2]^{\cdot+}[TCNE]^{\cdot-}$. Structural and Magnetic Characterization of Decamethylferrocenium Tetracyanoethenide, $[Fe(C_5Me_5)_2]^{\cdot+}[TCNE]^{\cdot+}\cdot MeCN$, and Decamethylferrocenium Pentacyanopropenide, $[Fe(C_5Me_5)_2]^{\cdot+}[C_3(CN)_5]^-$

Joel S. Miller,*[1a] Joseph C. Calabrese,[1a] Heiko Rommelmann,[1b] Sailesh R. Chittipeddi,[1c] Jian H. Zhang,[1d] William M. Reiff,*[1d] and Arthur J. Epstein*[1e]

Contribution from the Central Research and Development Department, E. I. du Pont de Nemours and Co., Inc., Experimental Station E328, Wilmington, Delaware 19898, Xerox Webster Research Center, Webster, New York 14580, Department of Physics and Department of Chemistry, The Ohio State University, Columbus, Ohio 43210-1106, and Department of Chemistry, Northeastern University, Boston, Massachusetts 02115. *Received June 3, 1986*

Abstract: The reaction of decamethylferrocene, $Fe(C_5Me_5)_2$, and tetracyanoethylene, TCNE, leads to the isolation of two products: $[Fe(C_5Me_5)_2]^{\cdot+}[TCNE]^{\cdot-}$ and $[Fe(C_5Me_5)_2]^{\cdot+}[C_3(CN)_5]^-$. Crystals of the $[TCNE]^{\cdot-}$ salt as the MeCN solvate belong to the monoclinic $C2/c$ space group [a = 16.250 (3) Å; b = 10.415 (2) Å, c = 32.851 (9) Å, β = 101.76 (2)°, Z = 8, V = 5443 Å^3]. The salt's linear chain motif is comprised of alternating $S = {}^1/_2$ cations and $S = {}^1/_2$ anions. The C_5 ring $[TCNE]^{\cdot-}$ separation is 3.51 Å, whereas the intrachain Fe(III)-Fe(III) separation is 10.415 Å. The cation's average Fe-C, C-C, and C-Me distances of 2.086, 1.410, and 1.499 Å agree with similar structural determinations. The $[TCNE]^{\cdot-}$ metric parameters are reported for the first time: central C-C, C-CN, and C≡N distances are 1.392 (9), 1.417 (2), and 1.140 (4) Å, respectively. The NC-C-CN angle is 117.7°. MeCN is lost upon isolation of the crystals, and the lattice transforms into an orthorhombic $Cmc2_1$ lattice. This desolvated complex can be prepared from THF and possesses chains of alternating cations and disordered anions. Adjacent chains are in-registry and out-of-registry as observed for the MeCN solvate. The $[C_3(CN)_5]^-$ salt belongs to the same space group [a = 13.950 (2) Å, b = 14.160 (2) Å, c = 12.870 (2) Å, β = 100.35 (1)°, Z = 4, V = 2501 Å^3], and the motif is comprised of alternating $S = {}^1/_2$ cations and $S = 0$ anions. The C_5-$[C_3(CN)_5]^-$ separation is 3.44 Å, and the intrachain Fe(III)-Fe(III) separation is 10.305 Å. The cations average Fe-C, C-C, and C-Me separations are 2.095, 1.423, and 1.501 Å, respectively. The anions average C-C, C-CN, and C≡N distances are 1.396 (2), 1.433, and 1.147 Å, respectively. The C-C-C, NC-C-CN, and NC-C-C angles are 129.7, 116.6, and 115.2°, respectively. The magnetic properties of these salts were measured via the Faraday technique. Above 2 K the antiferromagnetic $[Fe(C_5Me_5)_2]^{\cdot+}[C_3(CN)_5]^-$ and $[Co(C_5Me_5)_2]^+[TCNE]^{\cdot-}$ salts obey the Curie-Weiss expression, $\chi = C/(T-\theta)$, with a small θ ($[Co(C_5Me_5)_2]^+[TCNE]^{\cdot-}$: θ = −1.0 ± 0.3 K; μ_{eff} (calculated from $2.83(\chi T)^{1/2}$ from the high temperature data) = 1.72 μ_B; $[Fe(C_5Me_5)_2]^{\cdot+}[C_3(CN)_5]^-$: θ = −1.2 ± 0.4 K; μ_{eff} = 2.99 μ_B]. In contrast, above 60 K the $[Fe(C_5Me_5)_2]^{\cdot+}[TCNE]^{\cdot-}$ salt is ferromagnetic as it obeys the Curie-Weiss expression with a θ = +30 K; μ_{eff} evaluated at 300 K is 3.10 μ_B. The saturation magnetization of polycrystalline samples of the $[TCNE]^{\cdot-}$ salt at 4.2 K is 1.1 ± 0.1 × 10^4 emu·G/mol for 300 G < H < 80 000 G. For T > 17 K susceptibility data fit a 1-D $S = {}^1/_2$ Heisenberg ferromagnetic model. Below 5 K the charge-transfer salt displays the onset of *spontaneous magnetization in zero applied field consistent with a 3-D (bulk) ferromagnetic ground state.* For $[Fe(C_5Me_5)_2]^{\cdot+}[TCNE]^{\cdot-}$ the ^{57}Fe Mossbauer spectra exhibit a narrow singlet ($\Gamma \sim 0.323$ mm/s) with an isomer shift of 0.427 mm/s at room temperature. Zero field Zeeman split spectra are seen below 20 K. Anomously large internal fields varying from 382.1 kG at 9 K to 425.6 kG at 4.23 K are observed. A qualitative model based on the mixing of an excited state with the ground state for stabilizing ferromagnetic coupling and leading to bulk ferromagnetism is discussed.

Since the revelation that various TCNQ (TCNQ = 7,7,8,8-tetracyano-*p*-quinodimethane) salts form conducting linear chain, 1-D, phases,[2] interdisciplinary efforts have successfully sought to understand this class of materials.[3-6] While seeking to prepare new conducting phases, we prepared and characterized the 1-D phase of $[Fe(C_5Me_5)_2]^{\cdot+}[TCNQ]^{\cdot-}$ and found it to exhibit metamagnetism,[7] i.e., application of ~1.6 kG applied field switches the antiferromagnetic ground state ($T_{Neél}$ ~2.55 K) to an aligned moment state. With this precedent we set the deliberate goal of preparing a molecular based ferromagnetic complex. In the mid 1960's McConnell supplied some theoretical insight into stabilizing molecular based ferromagnetic materials. In 1963[8] he proposed that if radicals (especially odd-alternate) possessing large positive and negative π-spin densities were properly aligned (i.e., enabling the positive spin densities to exchange couple with negative spin densities on neighboring atoms), they might give rise to ferromagnetic exchange.[8,9] Mataga[10] and Ovchinnikov[11] subsequently suggested that high spin multiplicity polyradicals could lead to organic ferromagnets. Although structures based on polyradicals were proposed, mechanistic insight for achieving

(1) (a) Contribution No. 4097 Du Pont Co. (b) Xerox Corporation. (c) Department of Physics, The Ohio State University. (d) Northeastern University. (e) Department of Physics and Department of Chemistry, The Ohio State University, Columbus, OH (some of the preliminary work was carried out at the Xerox Webster Research Center).

(2) Acker, D. S.; Harder, R. J.; Hertler, W. R.; Mahler, W.; Melby, L. R.; Benson, R. E.; Mochel, W. E. *J. Am. Chem. Soc.* **1960**, *82*, 6408. Kepler, R. G.; Biersted, P. E.; Merrifield, R. E. *Phys. Rev. Lett.* **1960**, *5*, 503.

(3) Simon, J.; Andrê, J. J. *Molecular Semiconductors*; Springer Verlag: New York, 1985.

(4) Epstein, A. J.; Miller, A. J. *Sci. Am.* **1979**, *240*(#4), 52-61. Bechgaard, K.; Jerome, D. *Sci. Am.* **1982**, 247(#2), 52-61.

(5) *Extended Linear Chain Compounds*; Miller, J. S., Ed.; Plenum: New York; Vol. 1 and 2, 1982; Vol. 3, 1983.

(6) For detailed overview, see the proceedings of the recent series of international conferences: (a) Pecile, C.; Zerbi, G., Bozio, R., Girlando, A., Eds. *Mol. Cryst. Liq. Cryst.* **1985**, 117-121. (b) Comes, R., Bernier, P., Andrê, J. J., Rouxel, J., Eds. *J. Phys., Colloq. (Paris)* **1983**, *44-C3*. (c) Epstein, A. J., Conwell, E. M., Eds. *Mol. Cryst. Liq. Cryst.* **1981**, 77, 79, 82, 83, 85 and 86. (d) Carneiro, K., Ed. *Chem. Scr.* **1981**, 17. (e) Bartsic, S., Bjelis, A., Cooper, J. R., Leontic, B. A., Eds. *Lecture Notes Physics* **1979**, 95 and 96. (f) Miller, J. S., Epstein, A. J., Eds. *Ann. N. Y. Acad. Sci.* **1978**, *313*.

(7) Candela, G. A.; Swarzendruber, L.; Miller, J. S.; Rice, M. J. *J. Am. Chem. Soc.* **1979**, *101*, 2755-2756.

(8) McConnell, H. M. *J. Phys. Chem.* **1963**, *39*, 1910.

(9) Buchachenko, A. L. *Dokl. Akad. Nauk SSSR* **1979**, *244*, 1146-1148.

(10) Mataga, N. *Theor. Chim. Acta* **1968**, *10*, 372-376.

(11) Ovchinnikov, A. A. *Theor. Chim. Acta* **1978**, *47*, 297-304. Ovchinnikov, A. A. *Dokl. Akad. Nauk SSSR* **1977**, *236*, 928-931.

0002-7863/87/1509-0769$01.50/0

macroscopic ferromagnetic behavior from $S > {}^1/_2$ radicals (microscopically ferromagnetically coupled) was not elucidated in detail. Recently, a dilute thermally unstable nonet state polyradical has been characterized to exhibit antiferromagnetic coupling but not ferromagnetism.[12,13]

An alternate approach based on charge-transfer complexes was proposed by McConnell[14] and later expanded upon by Breslow.[15] This model requires 1-D chains of alternating $S = {}^1/_2$ donors, D, and acceptors, A, i.e., $\cdots D^{\bullet+}A^{\bullet-}D^{\bullet+}A^{\bullet-}\cdots$, such that upon charge transfer a triplet is formed and thus ferromagnetic coupling may result. The metallocenes and bis(arene)metal complexes we are studying possess the appropriate motif as well as electronic structure to test aspects of this model. Thus, with this theoretical encouragement we have undertaken the systematic study of metallocenes (primarily decamethylferrocene) and bisarenemetal complexes of principally planar polycano anions. We have reported on the $[C(CN)_3]^-$,[16] $[TCNQ]^{\bullet-}$,[7,17] and $[DDQ]^{\bullet-}$[18] [DDQ = 2,3-dichloro-4,5-dicyanobenzoquinone] salts of $[Fe(C_5Me_5)_2]^{\bullet+}$. Herein we report the structures and properties of the $[TCNE]^{\bullet-}$ and $[C_3(CN)_5]^-$ salts of $[Fe(C_5Me_5)_2]^{\bullet+}$ with specific emphasis on the bulk ferromagnetic properties observed for the $[TCNE]^{\bullet-}$ salt. With these results and our ongoing studies we look forward to elucidating the key electronic and steric features which stabilize ferromagnetic behavior and will ultimately guide us toward the synthesis of organic and possibly polymeric ferromagnetic materials. Our current thinking on the mechanism of spin exchange leading to bulk ferromagnetic behavior is also discussed.

Experimental Section

Synthesis. Decamethylferrocene was used as obtained from either Strem Chemicals (Newburyport, MA) or Organometallics, Inc. (E. Hampstead, NH). Decamethylcobaltocenium hexafluorophosphate (Strem) was converted to $Co(C_5Me_5)_2$ by a literature proceudre.[19a] TCNE was obtained from Du Pont archives and was sublimed prior to use. The $[NEt_4][C_3(CN)_5]$ salt[19b] was an appreciated gift from O. Webster. Acetonitrile was distilled twice (P_2O_5, CaH_2) under argon, and TCNE was sublimed prior to use. Tetrahydrofuran, THF, was distilled from sodium benzophenone under argon. All syntheses were carried out in a Vacuum Atmosphere HE501 inert atmosphere box.

$[Fe(C_5Me_5)_2]^{\bullet+}[TCNE]^{\bullet-}\cdot MeCN$. Dark green needle crystals of this charge-transfer salt were prepared via low-temperature crystallization of an acetonitrile solution containing the neutral donor and acceptor. In a typical preparation $Fe(C_5Me_5)_2$ (2.70 g, 8.274 mmol) dissolved in 300 mL of hot MeCN was added to TCNE (1.06 g, 8.274 mmol) dissolved in 5 mL of acetonitrile. After boiling off one-half of the solvent the solution was refrigerated overnight at −30 °C. The black long needle crystals which formed were harvested via vacuum filtration. All operations were undertaken within the inert atmosphere box. The product tended to dissolved upon warming, thus rapid collecting while cold resulted in the greatest yields (6.82 mmol, 82%). Crystals in equilibrium with the supernate were determined by X-ray diffraction to contain 1 equiv of MeCN (vide infra) per Fe. Crystals, although ca. 1 cm long and appearing nicely formed, lost MeCN upon isolation and were judged to be polycrystalline by X-ray analysis [elemental Anal. Calcd for $[Fe(C_5Me_5)_2][TCNE]\cdot MeCN$ ($C_{28}H_{33}FeN_5$): C, 67.88; H, 6.71; N, 14.13; and Fe, 11.27. Anal. Calcd for $[Fe(C_5Me_5)_2][TCNE]$ ($C_{26}H_{30}FeN_4$): C, 68.72; H, 6.65; N, 12.33; and Fe, 12.29. Found: C, 68.94; 68.74, and, 68.88; H, 6.60, 6.70, and 6.54; N, 12.32, 12.35, and 12.28; and Fe, 12.09, 12.22, and 12.28. Vibrational spectra (Nujol) ν_{CN} = 2183 m and 2144 s; (Fluorolube) ν_{CN} = 2183 m, and 2144 s]. Acetonitrile solutions of this complex exhibit multiple absorptions between 20 000 and 28 500 cm^{-1}. The IR and UV spectra are characteristic for $[TCNE]^{\bullet-}$.[20,21] Guinier powder data, d(I): 7.01 (100), 7.27 (80), 3.46 (19), 3.37 (18), 8.79 (17), 7.98 (15), and 3.51 Å (15). The orthorhombic unit cell parameters obtained from the powder data are a = 10.59 Å, b = 16.02 Å, c = 14.46 Å, V = 2453 Å^3. The desolvated sample may also be prepared from THF via slow diffusion. In a three compartment cell was placed 1.00 g $Fe(C_5Me_5)_2$ (3.06 mmol) dissolved in 10 mL of THF, and 0.40 g of TCNE (3.06 mmol) dissolved in 10 mL of THF. After standing for 100 h 0.46 g (33%) of the product was isolated. The cell constants refined from the powder diffraction data were a = 10.606 (10) Å, b = 16.184 (10) Å, c = 14.597 (12) Å, and V = 2506 Å^3. Single crystals were determined to belong to the orthorhombic $Cmc2_1$ space group (at −40 °C: a = 10.602 (2) Å, b = 16.098 (4) Å, c = 14.565 (1) Å, V = 2486 Å^3; at room temperature: a = 10.620 (1), 10.613 (2) Å, b = 16.100 (4), 16.102 (3) Å, c = 14.580 (1), 14.580 (2) Å, and V = 2493, 2492 Å^3).[22] Thus, the THF grown crystals were identical with those prepared from MeCN after the solvent was lost. Elemental Anal. Found: C, 68.92; H, 6.54; and N, 12.49. Vibrational spectrum (Nujol) ν_{CN} = 2183 m and 2144 s cm^{-1}.

$[Co(C_5Me_5)_2]^+[TCNE]^{\bullet-}$. Yellow-orange needle crystals of this charge-transfer salt were prepared at low temperature. In a typical preparation $Co(C_5Me_5)_2$ (120 mg, 0.364 mmol) dissolved in 30 mL of hot acetonitrile. To this solution was added 47 mg (0.364 mmol) of TCNE dissolved in 5 mL of MeCN. After boiling off all but ~2 mL of the solvent, the solution was refrigerated overnight at −25 °C. The needle crystals (124 mg, 74%) were harvested via vacuum filtration [Elemental Anal. Calcd for $[Co(C_5Me_5)_2][TCNE]$ ($C_{26}H_{30}N_4Co$): C, 68.21; H, 6.61; N, 12.25; Co, 12.88. Found: C, 68.22; H, 6.69; N, 12.21; ν_{CN} (Fluorolube) = 2183 s, 2144 s cm^{-1} (Fluorolube). Guinier powder data, d (I): 7.04 (100) and 7.31 (68) Å]. Crystals enabling the single crystal unit cell determination were unable to be grown. Apparent single crystals, like the Fe^{III} analogue, lost solvents and diffracted like a powder. Attempts to grow crystals in a capillary from a saturated solution at low temperature via the technique described above for the Fe^{III} analogue were unsuccessful.

$[Fe(C_5Me_5)_2]^{\bullet+}[BF_4]^-$. This emerald green salt was prepared via oxidation of $Fe(C_5Me_5)_2$ with benzoquinone in the presence of fluorboric acid. To 1.40 g of benzoquinone (13.0 mmol) dissolved in 20 mL of diethylether was added 9.84 g of 48% HBF_4. Subsequently, 8.45 g of $Fe(C_5Me_5)_2$ dissolved in 80 mL of diethyl ether was added. Upon standing essentially a quantitative yield of the product formed and was collected by vacuum filtration. The crystal habit was that of thin platelets. The unit cell was determined to belong to the monoclinic $P2/n$ space group (a = 13.85, b = 8.59, c = 8.82 Å, β = 106.46°, V = 1006 Å^3). ^1H NMR exhibits a contact shifted singlet resonance at −36.9 ppm relative to $SiMe_4$ in $CDCl_3$. The half-width at half-height is 0.55 ppm.

$[Fe(C_5Me_5)_2]^{\bullet+}[C_3(CN)_5]^-$. Dark purple chunky crystals of this composition were prepared via the reaction of equimolar amounts $[Fe(C_5Me_5)_2]^{\bullet+}[BF_4]^-$ and $[NEt_4]^+[C_3(CN)_5]^-$ in acetonitrile solution. Upon standing overnight at −8 °C crystals formed which were collected via vacuum filtration [Elemental Anal. Calcd for $C_{28}H_{30}FeN_5$: C, 68.30; H, 6.14; N, 14.22; Fe, 11.34. Found: C, 68.62, 68.63; H, 6.04, 5.95; N, 14.43, 14.50]. This complex was alternately prepared via recrystallization of the $[TCNE]^{\bullet-}$ salt from acetonitrile under ambient conditions. The IR infrared spectrum (Nujol ν_{CN} = 2196 s, ν_{CCC} = 1500 s cm^{-1}) is consistent with the presence of the $[C_3(CN)_5]^-$ ion.[20,23]

Physical Properties. Electronic absorption and vibrational spectra were recorded on Cary 2300 and Perkin Elmer 283B spectrophotometers, respectively. Magnetic susceptibility was determined by the Faraday method by using a previously described system.[18a] Elemental analyses were performed by Galbraith Laboratories (Knoxville, TN). Zero field Mossbauer spectra were determined by using a conventional constant acceleration spectrometer with a source of 150 mCurie ^{57}Co electroplated

(12) Sugawara, T.; Bandow, S.; Kimura, K.; Iwamura, H. *J. Am. Chem. Soc.* **1984**, *106*, 6449–6450. Iwamura, H.; Sugawara, T.; Itoh, K.; Takui, T. *Mol. Cryst. Liq. Cryst.* **1985**, *125*, 251–260. Sugawara, T.; Bandow, S.; Kimura, K.; Iwamura, H.; Itoh, K. *J. Am. Chem. Soc.* **1986**, *108*, 368–371. Iwamura, H. *Pure Appl. Chem.* **1986**, *58*, 187–196.

(13) At higher concentrations antiferromagnetic interactions are observed.[12]

(14) McConnell, H. M. *Proc. Robert A. Welch Found. Chem. Res.* **1967**, *11*, 144–145.

(15) Breslow, R. *Pure Appl. Chem.* **1982**, *54*, 927–938. Breslow, R.; Jaun, B.; Kluttz, R. Q.; Xia, C.-Z. *Tetrahedron* **1982**, *38*, 863–867. Breslow, R. *Mol. Cryst. Liq. Cryst.* **1985**, *125*, 261–267.

(16) Dixon, D. A.; Calabrese, J. C.; Miller, J. S. *J. Am. Chem. Soc.* **1986**, *108*, 2582–2588.

(17) Miller, J. S.; Reiff, W. M.; Zhang, J. H.; Dixon, D. A.; Preston, L. D.; Reis, A. H., Jr.; Gebert, E.; Extine, M.; Troup, J.; Epstein, A. J.; Ward, M. D., submitted for publication.

(18) (a) Gebert, E.; Reis, A. H., Jr.; Miller, J. S.; Rommelmann, H.; Epstein, A. J. *J. Am. Chem. Soc.* **1982**, *104*, 4403–4410. (b) Miller, J. S.; Krusic, P. J.; Dixon, D. A.; Reiff, W. M.; Zhang, Z. H.; Anderson, E. C.; Epstein, J. *J. Am. Chem. Soc.* **1986**, *108*, 4459–4466.

(19) (a) Robbins, J. L.; Edelstein, M.; Spencer, B.; Smart, J. C. *J. Am. Chem. Soc.* **1982**, *104*, 1882–1893. (b) Middleton, W. J.; Little, E. L.; Coffman, D. D.; Englehardt, V. A. *J. Am. Chem. Soc.* **1958**, *80*, 2795–2806.

(20) Similar ν_{CN} are reported in KBr;[21a] however, we noted decomposition as evidenced by a multiplet of ν_{CN} absorption for both the $[TCNE]^{\bullet-}$ and $[C_3(CN)_5]^-$ salts of $[Fe(C_5Me_5)_2]^{\bullet+}$ in dried KCl. Thus, we report the data obtained in Nujol and Fluorlube mulls.

(21) (a) Webster, O. W.; Mahler, W.; Benson, R. E. *J. Am. Chem. Soc.* **1962**, *84*, 3678–3684. (b) Rettig, M. F.; Wing, R. M. *Inorg. Chem.* **1969**, *8*, 2685–2689.

(22) Oneida Research Services, Inc., Whitesboro, NY 13492. Molecular Structure Corporation, College Station, TX 77840.

(23) (a) Hipps, K. W.; Geiser, V.; Mazur, U.; Willett, R. D.; *J. Phys. Chem.* **1984**, *88*, 2498–2507. (b) Dixon, D. A.; Miller, J. S., manuscript in preparation.

Table I. Fractional Coordinates ($\times 10^3$) and Isotropic Thermal Parameters for $[Fe(C_5Me_5)_2][C_3(CN)_5]$

atom	x	y	z	B_{iso}
Fe(1)	2500	2500	0	1.2 (1)′
N(1)	0	4789 (2)	2500	3.3 (1)′
N(2)	1805 (2)	3565 (2)	4656 (2)	3.7 (1)′
N(3)	838 (2)	748 (2)	3567 (2)	3.5 (1)′
C(1)	1682 (2)	1619 (1)	838 (2)	1.5 (1)′
C(2)	2276 (2)	2238 (2)	1547 (2)	1.9 (1)′
C(3)	2009 (2)	3183 (2)	1238 (2)	2.2 (1)′
C(4)	1253 (2)	3144 (2)	338 (2)	2.0 (1)′
C(5)	1049 (2)	2175 (2)	88 (2)	1.5 (1)′
C(6)	1701 (2)	562 (2)	894 (2)	2.6 (1)′
C(7)	3034 (2)	1938 (3)	2473 (2)	3.6 (1)′
C(8)	2436 (3)	4063 (2)	1788 (3)	4.5 (1)′
C(9)	726 (2)	3965 (2)	−236 (3)	4.0 (1)′
C(10)	288 (2)	1799 (2)	−785 (2)	2.8 (1)′
C(11)	0	2958 (2)	2500	1.8 (1)′
C(12)	0	3983 (2)	2500	2.2 (1)′
C(13)	670 (1)	2539 (2)	3304 (2)	2.0 (1)′
C(14)	1301 (2)	3104 (2)	4049 (2)	2.4 (1)′
C(15)	757 (2)	1544 (2)	3435 (2)	2.3 (1)′
H(6)	2352 (23)	338 (20)	1129 (24)	4.3 (7)
H(6′)	1463 (22)	276 (21)	213 (26)	4.7 (8)
H(6″)	1318 (24)	372 (22)	1372 (26)	5.1 (8)
H(7)	2756 (24)	1885 (23)	3079 (27)	5.3 (8)
H(7′)	3469 (29)	1390 (29)	2302 (31)	7.7 (11)
H(7″)	3498 (27)	2437 (25)	2586 (27)	5.9 (9)
H(8)	3161 (29)	4022 (26)	2005 (29)	6.7 (10)
H(8′)	2336 (26)	4619 (24)	1204 (30)	6.5 (10)
H(8″)	2121 (25)	4216 (24)	2315 (29)	5.9 (9)
H(9)	581 (26)	3895 (26)	−1003 (30)	6.2 (10)
H(9′)	1149 (23)	4525 (22)	−128 (25)	4.9 (8)
H(9″)	156 (24)	4114 (21)	37 (27)	5.0 (8)
H(10)	435 (25)	1141 (27)	−1034 (28)	6.3 (9)
H(10′)	−348 (22)	1825 (20)	−577 (23)	4.2 (7)
H(10″)	249 (21)	2237 (20)	−1414 (24)	4.2 (7)

onto the surface and annealed into the body of a 6-μm thick foil of high purity rhodium. The details of cryogenics, temperature control, etc. have been described previously.[24]

Collection and Reduction of X-ray Data—$[Fe(C_5Me_5)_2]^+[C_3(CN)_5]^-$. The crystal structure data were obtained from a purple reflecting irregular block (0.35 × 0.25 × 0.40 mm) cut from a larger crystal and placed on a SYNTEX R3 diffractometer equipped with a Mo Kα source, graphite monochrometer and LT1 low-temperature device operating at −100 °C. Preliminary diffractometer routines indicate a monoclinic cell with space group $C2/c$ and lattice constants a = 13.950 (2) Å, b = 14.160 (2) Å, c = 12.870 (2) Å, β = 100.35 (1)° as determined from 25 reflections. The volume of the unit cell is 2501.0 Å^3.

With Z = 4 the calculated density is 1.309 g/cm^3, and the absorption coefficient μ = 6.259 cm^{-1}. A total of 3149 data was collected with ω-scans from $4 < 2\theta < 55°$ yielding 2145 reflections with $I \geq 2\sigma(I)$ for the analysis. There was no variation of the intensities of the standard reflections during the data collection. The data were reduced in the usual fashion and phased via an automated Patterson routine. The pseudo F-centering in the data is consistent with the site symmetry of the solution, the cation lying on a center of symmetry, and the anion on a twofold axis. The intensities were corrected for absorption (DIFABS).[25a] The weights are proportional to $[\sigma^2(I) + 0.0009I^2]^{-1/2}$. A total of 217 parameters was refined with all non-hydrogen atoms refined anisotropically and all hydrogen atoms fixed. The final value for R_1 is 0.036 with R_w = 0.039 with an error of fit of 1.49. The high quality of the data is apparent from the successful isotropic refinement of the methyl hydrogen atoms. The largest peak on the final difference Fourier is 0.23 e$^-$/Å^3 near the Fe.

$[Fe(C_5Me_5)_2]^{\bullet+}[TCNE]^{\bullet-}$·MeCN. All attempts to collect data on single crystals obtained from solution crystallization were unsuccessful due to rapid loss of solvent. A single crystal suitable for data collection was grown from a CH_3CN solution in a sealed capillary within a CAD4 diffractometer at 5 °C by using an FTS LT1 refrigeration device. The grown crystal had approximate dimensions 0.25 × 0.25 × 0.25 mm. All further work was carried out at −30 °C. The diffractometer was equipped with a Mo Kα source and graphite monochrometer. The preliminary search routines indicated a monoclinic cell $C2/c$ with lattice constants a = 16.250 (3) Å, b = 10.415 (2) Å, c = 32.851 (9) Å, and β = 101.76 (2)° (V = 5433.0 Å^3) which were verified by axial photographs along each axis. With Z = 8, the calculated density is 1.208 g/cm^3 and μ = 5.746 cm^{-1}. The width at half-height of a typical ω-scan was 0.20°. Data were collected from $4 < 2\theta < 50°$ by using the ω-scan method where the scan width was determined by 0.80 + 0.35tan θ. A total of 5215 reflections was collected yielding 2062 reflections with $I > 3\sigma(I)$ which were used for the solution and refinement. There was slight (5%) intensity fluctuation which was adjusted by linear interpolation of the standard intensities.

After the usual adjustments for Lorentz polarization effects, the phases were obtained by direct methods (MULTAN).[25b] The solution shows sheets of cations and anions separated by sheets of CH_3CN solvent molecules. Loss of the loosely bound solvent explains the instability of crystals separated from the mother liquor. Hydrogen atoms were idealized from positions obtained by difference Fourier maps. The coordinates were refined via full-matrix anisotropic least squares on F which converged with R_1 = 0.059 and R_w = 0.054. Due to the small (3%) fluctuation of intensity around a typical diffraction vector (ψ-scan) effects of absorption were ignored. Scattering factors were from standard tables[26] including anomalous terms for Fe. The weights are proportional to $[\sigma^2(I) + 0.0009I^2]^{-1/2}$. A total of 307 parameters were refined to all non-hydrogen atoms refined anisotropically and all hydrogen atoms fixed. The error of fit is 1.62. One of the C_5Me_5 rings shows large thermal ellipsoids and may be partially disordered. The largest peak on the final difference, 0.16 e$^-$/Å^3, was located near the Fe with additional peaks near atom C(28).

Table II. Anisotropic Thermal Parameters (Å ×1000) $\exp[-19.739(U_{11}hha^*a^* \ldots + 2U_{12}hka^*b^* \ldots)]$ for $[Fe(C_5Me_5)_2][C_3(CN)_5]$

atom	U_{11}	U_{22}	U_{33}	U_{12}	U_{13}	U_{23}
Fe(1)	15.8 (2)	15.3 (2)	16.1 (2)	−0.2 (2)	3.0 (1)	−1.2 (2)
N(1)	61 (2)	25 (2)	38 (2)	0	2 (2)	0
N(2)	47 (1)	43 (1)	43 (1)	−6 (1)	−6 (1)	−2 (1)
N(3)	49 (1)	32 (1)	51 (1)	10 (1)	3 (1)	9 (1)
C(1)	18 (1)	20 (1)	20 (1)	−1 (1)	4 (1)	1 (1)
C(2)	18 (1)	37 (1)	16 (1)	−4 (1)	4 (1)	−2 (1)
C(3)	32 (1)	26 (1)	31 (1)	−9 (1)	18 (1)	−13 (1)
C(4)	28 (1)	19 (1)	33 (1)	5 (1)	15 (1)	5 (1)
C(5)	14 (1)	26 (1)	17 (1)	1 (1)	3 (1)	3 (1)
C(6)	41 (1)	20 (1)	41 (1)	2 (1)	14 (1)	8 (1)
C(7)	29 (1)	88 (2)	19 (1)	−6 (2)	−2 (1)	3 (1)
C(8)	66 (2)	49 (2)	67 (2)	−32 (2)	44 (2)	−40 (2)
C(9)	53 (2)	33 (1)	76 (2)	23 (1)	39 (2)	24 (2)
C(10)	21 (1)	56 (2)	24 (1)	−5 (1)	−4 (1)	2 (1)
C(11)	26 (2)	18 (1)	26 (2)	0	11 (1)	0
C(12)	30 (2)	29 (2)	23 (2)	0	3 (1)	0
C(13)	25 (1)	25 (1)	26 (1)	0 (1)	8 (1)	1 (1)
C(14)	32 (1)	30 (1)	30 (1)	2 (1)	7 (1)	5 (1)
C(15)	27 (1)	32 (1)	28 (1)	4 (1)	4 (1)	4 (1)

Table III. Interatomic Distances, Å, for $[Fe(C_5Me_5)_2][C_3(CN)_5]$

Fe(1)–C(1)	2.112 (2)	C(11)–C(13)	1.396 (2)
Fe(1)–C(2)	2.102 (2)	C(13)–C(14)	1.425 (3)
Fe(1)–C(3)	2.082 (2)	C(13)–C(15)	1.422 (4)
Fe(1)–C(4)	2.078 (2)	C(6)–H(6)	0.958 (30)
Fe(1)–C(5)	2.099 (2)	C(6)–H(6′)	0.968 (32)
N(1)–C(12)	1.142 (4)	C(6)–H(6″)	0.924 (32)
N(2)C(14)	1.155 (3)	C(7)–H(7)	0.933 (33)
N(3)–C(15)	1.143 (3)	C(7)–H(7′)	1.034 (40)
C(1)–C(2)	1.420 (3)	C(7)–H(7″)	0.951 (36)
C(1)–C(5)	1.422 (3)	C(8)–H(8)	1.000 (38)
C(1)–C(6)	1.500 (3)	C(8)–H(8′)	1.080 (36)
C(2)–C(3)	1.427 (4)	C(8)–H(8″)	0.899 (35)
C(2)–C(7)	1.505 (3)	C(9)–H(9)	0.976 (37)
C(3)–C(4)	1.420 (4)	C(9)–H(9′)	0.982 (32)
C(3)–C(8)	1.502 (3)	C(9)–H(9″)	0.950 (33)
C(4)–C(5)	1.427 (3)	C(10)–H(10)	1.017 (37)
C(4)–C(9)	1.498 (3)	C(10)–H(10′)	0.972 (30)
C(5)–C(10)	1.498 (3)	C(10)–H(10″)	1.014 (30)
C(11)–C(12)	1.451 (4)		

(24) Cheng, C.; Reiff, W. M. *Inorg. Chem.* **1977**, *16*, 2097.

(25) (a) Walker, N., Stuart, D. *Acta Crystallogr., Sect. A*: **1983**, *A39*, 158–166. (b) Main, P., Lessinger, L.; Woolfson, M. M.; Germain, G.; Declarq, J. P. MULTAN, York, England, and Louvain-la-Neuve, Belgium, 1978.

(26) *International Tables for X-ray Crystallography*; Kynoch Press: Birmingham, England, 1974; Vol. IV.

Table IV. Intramolecular Angles, deg, for $[Fe(C_5Me_5)_2][C_3(CN)_5]$

N(1)-C(12)-C(11)	180 (4)	C(2)-C(7)-H(7′)	113 (2)
N(2)-C(14)-C(13)	179.4 (5)	C(2)-C(7)-H(7″)	106 (2)
N(3)-C(15)-C(13)	178.3 (3)	C(3)-C(8)-H(8)	112 (2)
C(2)-C(1)-C(5)	108.3 (2)	C(3)-C(8)-H(8′)	107 (2)
C(2)-C(1)-C(6)	125.5 (2)	C(3)-C(8)-H(8″)	110 (2)
C(5)-C(1)-C(6)	126.1 (2)	C(4)-C(9)-H(9)	114 (2)
C(1)-C(2)-C(3)	107.9 (2)	C(4)-C(9)-H(9′)	109 (2)
C(1)-C(2)-C(7)	125.6 (2)	C(4)-C(9)-H(9″)	111 (2)
C(3)-C(2)-C(7)	126.6 (2)	C(5)-C(10)-H(10)	114 (2)
C(2)-C(3)-C(4)	108.0 (2)	C(5)-C(10)-H(10′)	110 (2)
C(2)-C(3)-C(8)	125.8 (3)	C(5)-C(10)-H(10″)	108 (2)
C(4)-C(3)-C(8)	126.1 (3)	H(6)-C(6)-H(6′)	107 (2)
C(3)-C(4)-C(5)	108.1 (2)	H(6)-C(6)-H(6″)	109 (3)
C(3)-C(4)-C(9)	126.8 (3)	H(6′)-C(6)-H(6″)	110 (3)
C(5)-C(4)-C(9)	125.1 (3)	H(7)-C(7)-H(7′)	118 (3)
C(1)-C(5)-C(4)	107.7 (2)	H(7′)-C(7)-H(7″)	108 (3)
C(1)-C(5)-C(10)	125.6 (2)	H(7′)-C(7)-H(7″)	100 (3)
C(4)-C(5)-C(10)	126.7 (2)	H(8)-C(8)-H(8′)	104 (3)
C(12)-C(11)-C(13)	115.2 (1)	H(8)-C(8)-H(8″)	114 (3)
C(13)-C(11)-C(13)[a]	129.7 (3)	H(8′)-C(8)-H(8″)	109 (3)
C(11)-C(13)-C(14)	120.7 (2)	H(9)-C(9)-H(9′)	104 (3)
C(11)-C(13)-C(15)	122.7 (2)	H(9)-C(9)-H(9″)	111 (3)
C(14)-C(13)-C(15)	116.6 (2)	H(9′)-C(9)-H(9″)	107 (3)
C(1)-C(6)-H(6)	111 (2)	H(10)-C(10)-H(10′)	112 (3)
C(1)-C(6)-H(6′)	112 (2)	H(10)-C(10)-H(10″)	107 (2)
C(1)-C(6)-H(6″)	108 (2)	H(10′)-C(10)-H(10″)	106 (2)
C(2)-C(7)-H(7)	110 (2)		

[a] $-x, y, {}^1/_2 - z$.

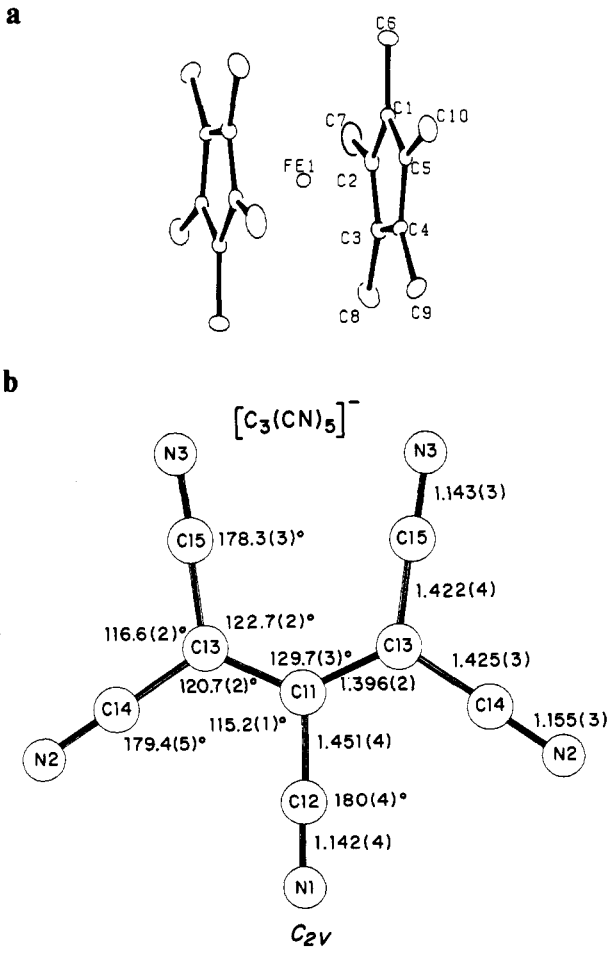

Figure 1. Atom labeling for $[Fe(C_5Me_5)_2]^{+}[C_3(CN)_5]^-$.

Results and Discussion

Structure Description. $[Fe(C_5Me_5)_2][C_3(CN)_5]$. The fractional coordinates, anisotropic thermal parameters, interatomic distances and angles as well as key intermolecular distances in the range of 3.4–3.6 Å are located in Tables I–V, respectively. Table VI lists the least-square planes. Atom labeling can be found in Figure 1, while Figure 2 depicts the unit cell. The staggered C_5 $[Fe(C_5Me_5)_2]^{+}$ cation is essentially equivalent to that observed for the $[TCNE]^{-}$ structure as well as others previously reported and is discussed with the description of the $[TCNE]^{-}$ structure, vide infra.

Table V. Intermolecular Distances <3.6 Å for $[Fe(C_5Me_5)_2][C_3(CN)_5]$[f]

N(1)···C(9)[c]	3.401 (4)
N(3)···C(6)[d]	3.544 (4)
N(3)···C(8)[e]	3.477 (4)
C(2)···C(13)	3.484 (3)
C(3)···C(11)	3.498 (2)
C(4)···C(11)	3.552 (2)
C(4)···C(13)[b]	3.560 (3)
C(5)···C(13)[b]	3.476 (3)
C(5)···C(15)[b]	3.531 (3)

[a] ${}^1/_2 - x, {}^1/_2 - y, -z$. [b] $-x, y, {}^1/_2 - z$. [c] $-x, 1 - y, -z$. [d] $x, -y, {}^1/_2 + z$. [e] ${}^1/_2 - x, -{}^1/_2 + y, {}^1/_2 - z$. [f] *a–e* are symmetry operation codes.

Table VI

Least-Squares Planes for $[Fe(C_5Me_5)_2][C_3(CN)_5]$

atom	deviation, Å
A. $[C_3(CN)_5]^-$—Plane 1	
N1	0.000
N3b	0.052
N2	0.020
C14b	−0.019
N3	−0.052
C15b	0.021
C11	0.000
C12	0.000
C13	0.005
C14	0.019
C15	−0.021
C13b	−0.005
N2b	−0.020
B. $-CC(CN)_2$ Group of $[C_3(CN)_5]^-$—Plane 2	
C11	−0.001
C13	0.004
C14	−0.001
C15	−0.001
C. $(NC)_2CC-$ Group of $[C_3(CN)_5]^-$—Plane 3	
C11	0.001
C13b	−0.004
C14b	0.001
C15b	0.001
D. C_5H_5 Ring of $[Fe(C_5Me_5)_2]^{+}$—Plane 4	
C1	−0.001
C2	0.001
C3	−0.001
C4	0.000
C5	0.000

Angles between Planes, deg

plane	1	2
2	0.95	
3	0.95	1.75

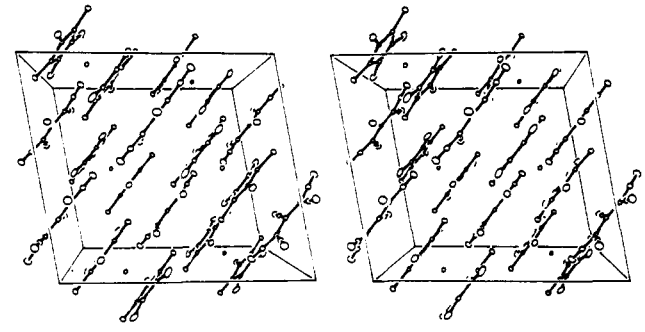

Figure 2. Stereoview of the unit cell of $[Fe(C_5Me_5)_2]^{+}[C_3(CN)_5]^-$.

Table VII. Structural Parameters for $[C_3(CN)_5]^{-a-c}$

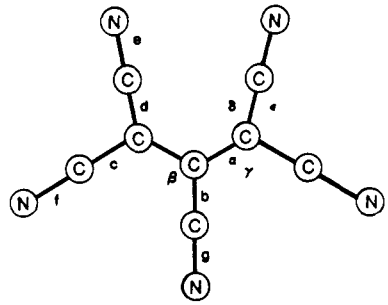

C–C	a	1.396 (2)	1.385	1.397
C–CN	b	1.451 (4)	1.454	1.454
C–CN	c	1.425 (3)	1.433	1.430
C–CN	d	1.422 (4)	1.421	1.415
C≡N	e	1.143 (3)	1.142	1.138
C≡N	f	1.155 (3)	1.148	1.143
C≡N	g	1.142 (4)	1.145	1.128
C–C–C	α	129.7 (3)	130.0	129.7
NC–C–C(CN)$_2$	β	115.2 (1)	115.8	115.2
C–C–CN	γ	120.7 (2)	120.7	119.9
C–C–CN	δ	122.7 (2)	123.5	119.9
NC–C–CN	ϵ	116.6 (2)	115.8	116.6
ref		this work	29	23a
T, °C		−100	21	19
R		3.6%	4.8%	4.7%

[a] Data from a significantly disordered structure has not been included.[27,28] [b] Distances in Å; angles in deg. [c] Uncorrected for thermal motion.

$[C_3(CN)_5]^-$. The planar C_{2v} anion lies on a twofold axis which passes through the central CCN group. There is a 1.75° dihedral angle between each $CC(CN)_2$ portion of the anion. The allyl C–C distance is 1.396 (2) Å. The C–CN distances range 1.451 (4) for the central one to ~1.423 Å for the exo ones. The C≡N bond lengths vary from 1.155 (3) (for N2–C14) to 1.142 Å for the remaining pair. The C–C–C, NC–C–CN, and NC–C–C angles are 129.7, 116.6, and 115.2°, respectively. These metric parameters are in accord with those reported for previous structures.[21b,27-29] The key distances and angles are located in Figure 1 and Table VII. Data from the severely disordered anions[27,28] previously reported have been neglected.

Solid-State Structures. The solid is comprised of alternating cations and anions. No significant interactions less than the sum of the van der Waal radii (3.4 Å) are observed, Table V. The intrachain Fe(III)–Fe(III) separation is 10.305 Å; however, several shorter interchain distances of 8.598, 9.567, and 9.939 Å are present. The $[C_3(CN)_5]^-$ plane and C_5 rings are parallel and separated by 3.44 Å. The Fe–N spacings less than the intrachain Fe–Fe separation of 10.305 Å range from 5.328 to 10.186 Å. The general stacking motif is essentially identical with that seen for the $[TCNQ]^{-\bullet}$,[17,30] $[DDQ]^{-\bullet}$,[18] and $[TCNE]^{-\bullet}$ salts (vide infra) of $[Fe(C_5Me_5)_2]^{+\bullet}$ as well as for $[Fe(C_5H_5)_2][TCNE]$.[31]

$[Fe(C_5Me_5)_2]^{+\bullet}[TCNE]^{-\bullet}\cdot MeCN$. The fractional coordinates, anisotropic thermal parameters, interatomic distances and angles, and least-square planes are tabulated in Tables VIII–XII, respectively. Table XIII summarizes the intramolecular distances <3.6 Å. Figures 3 and 4 contain the necessary atom labeling and steroview of the unit cell, respectively.

The $[Fe(C_5Me_5)_2]^{+\bullet}$ Cation. The radical cation is staggered with local C_5 symmetry and is essentially equivalent to that observed for the $[C_3(CN)_5]^-$ salt. The average Fe–C and C–C ring distances are 0.01 Å shorter for the $[TCNE]^{-\bullet}$ salt than the $[C_3(CN)_5]^-$ salt; whereas the average C–Me distances are essentially equivalent. Table XIV summarizes the important distances for a number of related materials. Relative to $Fe^{II}(C_5Me_5)_2$[32a] the cation possesses slightly longer Fe^{III}–C and Fe^{III}–C_5 ring centroid distances by ~0.04 Å; however, the C–C

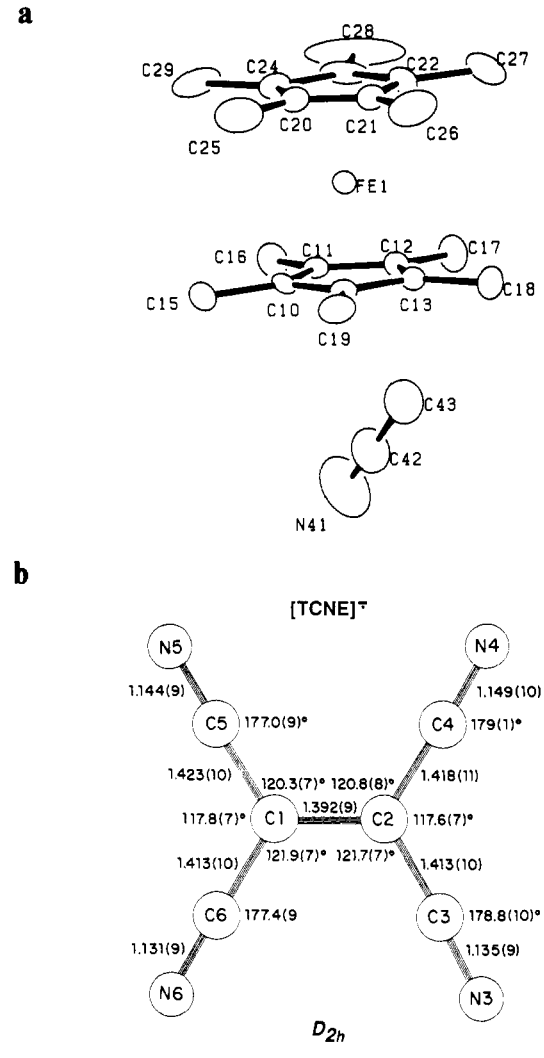

Figure 3. Atom labeling for $[Fe(C_5Me_5)_2]^{+\bullet}[TCNE^{-\bullet}\cdot MeCN$.

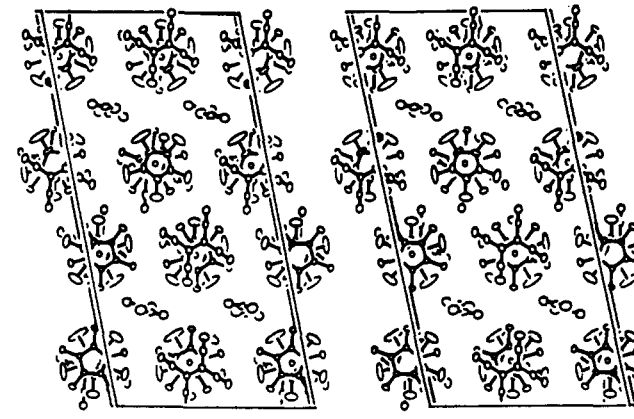

Figure 4. Stereoview of the unit cell along the b-axis for $[Fe(C_5Me_5)_2]^{+\bullet}[TCNE]^{-\bullet}\cdot MeCN$.

(27) Jensen, W. D.; Jacobson, R. A. *Inorg. Chem. Acta* **1981**, *50*, 189–194.
(28) Sim, G. A.; Woodhouse, D. I.; Knox, G. R. *J. Chem. Soc., Dalton Trans.* **1979**, 629–635.
(29) Bertolosi, V.; Gilli, G. *Acta Crystallogr., Sect. C: Cryst. Struct. Commun.* **1983**, *C39*, 1242–1245.
(30) Miller, J. S.; Reis, A. H., Jr.; Gebert, E.; Ritsko, J. J.; Salaneck, W. R.; Kovnat, L.; Cape, T. W.; Van Duyne, R. P. *J. Am. Chem. Soc.* **1979**, *101*, 7111.
(31) Adman, E.; Rosenblum, M.; Sullivan, S.; Marguilis, T. N. *J. Am. Chem. Soc.* **1967**, *89*, 4540–4542. Foxman, B., private communication.
(32) (a) Freyberg, D. P.; Robbins, J. L.; Raymond, K. N.; Smart, J. C. *J. Am. Chem. Soc.* **1971**, *93*, 892–897. (b) Lemerovskii, D. A.; Stukan, R. A.; Tarasevich, B. N.; Slovokhotov, Yu. L.; Antipin, M. Yu.; Kalinin, A. E.; Struchkov, Yu. T. *Koord. Khim.* **1981**, *7*, 240–249.

Table VIII. Fractional Coordinates ($\times 10^3$) and Isotropic Thermal Parameters for $[Fe(C_5Me_5)_2][TCNE]\cdot MeCN$

atom	x	y	z	B_{iso}
Fe(1)	4334.4 (6)	2250.8 (9)	1143.6 (3)	2.9 (1)′
N(3)	5947 (4)	−2626 (8)	601 (2)	6.8 (3)′
N(4)	5177 (5)	−2673 (9)	1805 (2)	8.2 (3)′
N(5)	2796 (4)	−2912 (8)	1248 (2)	6.5 (3)′
N(6)	3519 (4)	−2869 (9)	18 (2)	7.3 (3)′
N(41)	2158 (7)	8209 (13)	2460 (3)	13.2 (5)′
C(1)	3930 (5)	−2805 (8)	807 (3)	4.3 (2)′
C(2)	4769 (5)	−2713 (8)	1007 (3)	4.7 (3)′
C(3)	5423 (5)	−2653 (8)	783 (3)	5.0 (3)′
C(4)	4998 (5)	−2686 (9)	1448 (3)	5.7 (3)′
C(5)	3286 (5)	−2867 (8)	1043 (3)	4.8 (3)′
C(6)	3685 (5)	−2849 (10)	369 (3)	5.1 (3)′
C(10)	3683 (4)	3834 (6)	853 (2)	2.9 (2)′
C(11)	3613 (4)	3792 (6)	1278 (2)	2.9 (2)′
C(12)	4451 (4)	3871 (7)	1523 (2)	3.3 (2)′
C(13)	5019 (4)	3962 (6)	1248 (2)	3.0 (2)′
C(14)	4542 (5)	3945 (6)	834 (2)	3.1 (2)′
C(15)	2965 (5)	3842 (7)	486 (2)	4.6 (3)′
C(16)	2812 (5)	3740 (7)	1435 (2)	4.8 (3)′
C(17)	4677 (5)	3942 (8)	1994 (2)	5.1 (3)′
C(18)	5953 (4)	4118 (7)	1375 (2)	4.9 (3)′
C(19)	4900 (5)	4058 (7)	451 (2)	5.1 (3)′
C(20)	4251 (6)	625 (7)	767 (3)	4.6 (3)′
C(21)	5048 (5)	723 (7)	997 (3)	4.4 (3)′
C(22)	5006 (6)	651 (7)	1407 (3)	4.8 (3)′
C(23)	4146 (8)	542 (7)	1440 (3)	5.9 (4)′
C(24)	3670 (5)	529 (7)	1017 (3)	4.8 (3)′
C(25)	4025 (8)	625 (9)	298 (3)	9.8 (5)′
C(26)	5843 (6)	805 (9)	822 (4)	9.1 (4)′
C(27)	5744 (8)	662 (9)	1766 (4)	12.3 (5)′
C(28)	3836 (13)	407 (10)	1824 (5)	20.6 (10)′
C(29)	2739 (6)	380 (8)	868 (5)	13.4 (6)′
C(42)	2640 (8)	7559 (13)	2408 (3)	7.6 (5)′
C(43)	3286 (7)	6679 (10)	2340 (3)	8.6 (4)′
H(15)	2753	4690	436	8.0
H(15′)	2527	3295	539	8.0
H(15″)	3152	3540	247	8.0
H(16)	2882	3169	1665	8.0
H(16′)	2374	3440	1221	8.0
H(16″)	2682	4573	1520	8.0
H(17)	5175	3450	2093	8.0
H(17′)	4231	3602	2108	8.0
H(17″)	4778	4809	2080	8.0
H(18)	6179	3425	1549	8.0
H(18′)	6075	4905	1521	8.0
H(18″)	6193	4126	1135	8.0
H(19)	4537	3659	227	8.0
H(19′)	5437	3645	499	8.0
H(19″)	4968	4939	392	8.0
H(25)	3989	−237	202	8.0
H(25′)	4422	1086	190	8.0
H(25″)	3478	1016	214	8.0
H(26)	6258	1274	1005	8.0
H(26′)	5717	1223	559	8.0
H(26″)	6041	−40	787	8.0
H(27)	5894	−198	1838	8.0
H(27′)	5552	1055	1997	8.0
H(27″)	6177	1125	1699	8.0
H(28)	4066	−365	1658	8.0
H(28′)	3243	342	1757	8.0
H(28″)	4009	1116	1994	8.0
H(29)	2616	−475	770	8.0
H(29′)	2555	957	638	8.0
H(29″)	2453	569	1080	8.0
H(43)	3772	6810	2548	8.0
H(43′)	3404	6837	2075	8.0
H(43″)	3086	5828	2354	8.0

and C–Me distances remain the same. This trend is also observed for $Fe^{II}(C_5H_5)_2/[Fe^{III}(C_5H_5)_2]^{\bullet+}$.[33]

The $[TCNE]^{\bullet-}$ Anion. This is the first reported structural characterization of the D_{2h} $[TCNE]^{\bullet-}$; thus, its structural parameters are of theoretical interest.[34] The radical anion lies between essentially parallel C_5Me_5 rings which do not distort the ion. This is in contrast with the other previous report of $[TCNE]^{\bullet-}$ which exists substantially distorted as dimers in a segregated chain.[32b] The distances and angles are summarized in Figure 3. Relative to TCNE, the central C–C and C–CN bonds elongate by ~0.04 and ~0.02 Å, respectively; whereas the C≡N distance contracts by ~0.02 Å. Each monomer in the $S = 0$ $[TCNE]_2^{2-}$

(33) Sullivan, B. W.; Foxman, B. *Organometallics* **1983**, *2*, 187–189.

Table IX. Anisotropic Thermal Parameters (Å ×1000) $\exp[-19.739(U_{11}hha^*a^* \ldots + 2(U_{12}hka^*b^* \ldots))]$ for $[Fe(C_5Me_5)_2][TCNE]\cdot MeCN$

atom	U_{11}	U_{22}	U_{33}	U_{12}	U_{13}	U_{23}
Fe(1)	36 (1)	35 (1)	38 (1)	0 (1)	7 (1)	4 (1)
N(3)	58 (5)	91 (6)	116 (6)	−9 (5)	30 (4)	−4 (5)
N(4)	122 (7)	104 (7)	79 (6)	2 (6)	5 (5)	−4 (6)
N(5)	66 (5)	99 (6)	91 (5)	−1 (5)	34 (4)	1 (5)
N(6)	75 (5)	122 (7)	83 (5)	19 (5)	22 (5)	1 (7)
N(41)	165 (11)	230 (14)	109 (8)	92 (10)	33 (8)	−35 (8)
C(1)	49 (5)	45 (5)	72 (6)	5 (5)	17 (4)	5 (5)
C(2)	55 (5)	41 (5)	79 (6)	4 (5)	9 (5)	2 (5)
C(3)	46 (5)	48 (6)	93 (7)	−2 (5)	5 (5)	−8 (5)
C(4)	62 (6)	56 (6)	98 (8)	1 (5)	14 (6)	−5 (7)
C(5)	54 (5)	46 (5)	81 (6)	−2 (5)	12 (5)	7 (5)
C(6)	44 (5)	75 (6)	79 (6)	8 (5)	23 (5)	5 (8)
C(10)	45 (5)	29 (4)	32 (4)	10 (4)	2 (4)	5 (4)
C(11)	41 (5)	30 (4)	40 (5)	1 (4)	11 (4)	3 (4)
C(12)	39 (5)	43 (5)	43 (5)	1 (4)	11 (4)	4 (4)
C(13)	41 (5)	35 (5)	37 (5)	3 (4)	8 (4)	−2 (4)
C(14)	47 (5)	32 (5)	43 (5)	0 (4)	14 (4)	6 (4)
C(15)	64 (6)	55 (5)	49 (5)	4 (4)	−6 (4)	8 (4)
C(16)	46 (5)	78 (6)	62 (6)	8 (4)	21 (4)	6 (5)
C(17)	70 (6)	89 (7)	32 (5)	−1 (5)	3 (4)	−1 (4)
C(18)	38 (5)	70 (6)	75 (6)	−4 (4)	4 (4)	−2 (5)
C(19)	91 (7)	54 (5)	56 (6)	−8 (5)	31 (5)	3 (4)
C(20)	62 (6)	39 (5)	70 (7)	−3 (5)	2 (6)	2 (5)
C(21)	43 (6)	37 (5)	85 (7)	2 (4)	11 (5)	−1 (5)
C(22)	78 (7)	43 (6)	50 (6)	11 (5)	−10 (6)	4 (4)
C(23)	136 (10)	39 (6)	72 (7)	16 (6)	72 (7)	24 (5)
C(24)	41 (5)	42 (6)	104 (8)	−3 (4)	23 (6)	8 (5)
C(25)	214 (13)	67 (7)	81 (8)	5 (8)	8 (8)	−22 (6)
C(26)	86 (8)	71 (7)	208 (12)	0 (6)	75 (8)	−18 (7)
C(27)	202 (13)	62 (7)	150 (11)	36 (8)	−85 (10)	5 (7)
C(28)	584 (31)	55 (8)	242 (17)	36 (13)	320 (20)	45 (9)
C(29)	47 (7)	47 (7)	411 (21)	−11 (5)	39 (10)	12 (10)
C(42)	111 (10)	129 (13)	50 (6)	12 (8)	18 (6)	−9 (7)
C(43)	115 (9)	121 (9)	88 (8)	5 (8)	12 (7)	−14 (7)

Table X. Interatomic Distances, Å, for $[Fe(C_5Me_5)_2][TCNE]\cdot MeCN$

Fe(1)–C(10)	2.083 (6)	C(10)–C(14)	1.415 (8)
Fe(1)–C(11)	2.087 (7)	C(10)–C(15)	1.498 (8)
Fe(1)–C(12)	2.084 (7)	C(11)–C(12)	1.436 (8)
Fe(1)–C(13)	2.092 (7)	C(11)–C(16)	1.495 (8)
Fe(1)–C(14)	2.099 (7)	C(12)–C(13)	1.420 (8)
Fe(1)–C(20)	2.084 (8)	C(12)–C(17)	1.518 (9)
Fe(1)–C(21)	2.082 (8)	C(13)–C(14)	1.421 (8)
Fe(1)–C(22)	2.081 (8)	C(13)–C(18)	1.500 (9)
Fe(1)–C(23)	2.082 (8)	C(14)–C(19)	1.492 (9)
Fe(1)–C(24)	2.090 (8)	C(20)–C(21)	1.364 (10)
N(3)–C(3)	1.135 (9)	C(20)–C(24)	1.374 (10)
N(4)–C(4)	1.149 (10)	C(20)–C(25)	1.511 (11)
N(5)–C(5)	1.144 (9)	C(21)–C(22)	1.364 (10)
N(6)–C(6)	1.131 (9)	C(21)–C(26)	1.522 (11)
N(41)–C(42)	1.074 (12)	C(22)–C(23)	1.428 (11)
C(1)–C(2)	1.392 (9)	C(22)–C(27)	1.502 (11)
C(1)–C(5)	1.423 (10)	C(23)–C(24)	1.447 (11)
C(1)–C(6)	1.413 (10)	C(23)–C(28)	1.455 (12)
C(2)–C(3)	1.413 (10)	C(24)–C(29)	1.500 (11)
C(2)–C(4)	1.418 (11)	C(42)–C(43)	1.446 (13)
C(10)–C(11)	1.426 (8)		

(34) Molecular orbital calculations of the structure, vibrational frequencies, and where appropriate the charge and spin distributions for $[TCNE]^z$ (z = 0, 1–, 2–) will be the subject of another paper. Dixon, D. A.; Miller, J. S. *J. Am. Chem. Soc.*, in press.

Table XI. Intramolecular Angles[a] for $[Fe(C_5Me_5)_2][TCNE]\cdot MeCN$

N(3)–C(3)–C(2)	178.8 (10)	C(12)–C(13)–C(18)	125.5 (7)
N(4)–C(4)–C(2)	179 (1)	C(14)–C(13)–C(18)	126.3 (7)
N(5)–C(5)–C(1)	177.0 (9)	C(10)–C(14)–C(13)	108.0 (6)
N(6)–C(6)–C(1)	177.4 (9)	C(10)–C(14)–C(19)	127.0 (7)
N(41)–C(42)–C(43)	180 (2)	C(13)–C(14)–C(19)	125.1 (7)
C(2)–C(1)–C(5)	120.3 (7)	C(21)–C(20)–C(24)	111.4 (8)
C(2)–C(1)–C(6)	121.9 (7)	C(21)–C(20)–C(25)	125 (1)
C(5)–C(1)–C(6)	117.8 (7)	C(24)–C(20)–C(25)	123.8 (10)
C(1)–C(2)–C(3)	121.7 (7)	C(20)–C(21)–C(22)	108.0 (8)
C(1)–C(2)–C(4)	120.8 (8)	C(20)–C(21)–C(26)	125.4 (10)
C(3)–C(2)–C(4)	117.6 (7)	C(22)–C(21)–C(26)	126.5 (9)
C(11)–C(10)–C(14)	108.8 (6)	C(21)–C(22)–C(23)	109.1 (8)
C(11)–C(10)–C(15)	125.9 (7)	C(21)–C(22)–C(27)	126 (1)
C(14)–C(10)–C(15)	125.3 (7)	C(23)–C(22)–C(27)	125 (1)
C(10)–C(11)–C(12)	107.0 (6)	C(22)–C(23)–C(24)	105.4 (7)
C(10)–C(11)–C(16)	125.9 (6)	C(22)–C(23)–C(28)	126 (1)
C(12)–C(11)–C(16)	127.1 (6)	C(24)–C(23)–C(28)	128 (1)
C(11)–C(12)–C(13)	108.2 (6)	C(20)–C(24)–C(23)	106.0 (7)
C(11)–C(12)–C(17)	125.4 (7)	C(20)–C(24)–C(29)	126 (1)
C(13)–C(12)–C(17)	126.3 (7)	C(23)–C(24)–C(29)	128 (1)
C(12)–C(13)–C(14)	108.1 (6)		

[a] Degrees.

Table XII. Least-Squares Planes for $[Fe(C_5Me_5)_2][TCNE]\cdot MeCN$

atom	deviation, Å
A. $[TCNE]^{\cdot-}$—Plane 1	
N3	−0.010
N4	−0.009
N5	−0.001
N6	−0.002
C1	0.004
C2	0.009
C3	0.011
C4	0.004
C5	0.000
C6	−0.006
B. C_5Me_5 Ring of $[Fe(C_5Me_5)_2]^{\cdot+}$—Plane 2	
C10	−0.003
C11	0.001
C12	0.000
C13	−0.002
C14	0.003
C. C_5Me_5 Ring of $[Fe(C_5Me_5)_2]^{\cdot+}$—Plane 3	
C20	−0.009
C21	0.011
C22	−0.008
C23	0.003
C24	0.003

Table XIII. Intramolecular Distances <3.6 Å for $[Fe(C_5Me_5)_2][TCNE]\cdot MeCN$[c]

N(6)···N(6)[b]	3.378 (14)
C(17)···C(17)[a]	3.275 (14)

[a] $1-x, y, {}^1/_2-z$. [b] ${}^1/_2-x, -{}^1/_2-y, -z$. [c] *a* and *b* are symmetry operation codes.

dimer is nonplanar (i.e., bent 15° via a b_{3u} out-of-plane vibration), and the central C–C bond is essentially equivalent in length to that observed for TCNE. The C–CN and C≡N distances are, however, +0.03 and −0.03 Å different than observed for TCNE.[35] Infrared, Raman, and UV–vis as well as structural data for $[TCNE]^n$ (n = 0, 1−, and 2−) are compared to ab initio molecular orbital calculations in a subsequent paper.[34]

Solid-State Structure. Similar to the $[C_3(CN)_5]^-$ salt the solid consists of alternating radical cations and radical anions along the *b*-axis. The intrachain Fe(III)–Fe(III) separation is 10.415 Å which is 0.1 Å longer than observed for the $[C_3(CN)_5]^-$ salt. The intrachain Fe–Fe separation is >0.1 Å shorter than reported for the $[TCNQ]^{\cdot-}$[17] and $[DDQ]^{\cdot-}$[18a] salts, Table XIII. Interchain Fe(III)–Fe(III) separations less than the intrachain distance are 8.603, 8.732, 9.473, 9.651, and 10.028 Å. The C_5-ring-TCNE plane has a 2.8° dihedral angle, and its average separation is 3.51 Å. No unusual shorter than van der Waals contacts are evident in this structure. The acetonitrile of solvation lies in sheets parallel to the $\cdots D^{\cdot+}A^{\cdot-}D^{\cdot+}A^{\cdot-}\cdots$ (*b*-axis) chain. The MeCN's C≡N and C—Me distances are 1.074 (12) and 1.446 (13) Å, respectively. The C≡N is substantially shorter than the 1.14–1.16 Å reported for TCNE, $[C_3(CN)_5]^-$, and $[C(CN)_3]^-$.[16]

Since magnetic properties are a consequence of spin–spin interactions and the dominant spins on the cations and anions resides on the Fe(III) $e_{2g}(d_{x^2-y^2}/d_{xy})$[19a] and the N $b_{3g}(p_z)$[34] orbitals, vide infra, an understanding of the intra-and interchain nonbonding Fe–Fe, Fe–N, and N–N interactions is imperative in order to elucidate the mechanism of cooperative spin–spin interactions. Since cooperative magnetic interactions, when either or both the $S = {}^1/_2$ donor or $S = {}^1/_2$ acceptor comprising the $\cdots D^{\cdot+}A^{\cdot-}D^{\cdot+}A^{\cdot-}\cdots$ structure is replaced by similarly sized and charged $S = 0$ species, were not observed (vide infra), we limit our investigations to $[Fe(C_5Me_5)_2][TCNE]$ and the Fe–Fe, Fe–N, and N–N interactions to those less than the intrachain Fe–Fe distance, i.e., 10.415 Å.

As noted earlier the structure of the monoclinic MeCN solvate is not the structure of the material whose physical properties were measured. The loss of MeCN transforms this lattice into an orthorhombic unit cell. Crystals of $[Fe(C_5Me_5)_2][TCNE]$ possessing the identical lattice parameters and the $Cmc2_1$ space group can be prepared by slow diffusion in THF. Qualitatively, the structure consists of chains of alternating cations and anions as noted for the solvated phase; however, although the cation is ordered, the anion sitting midway between cations (and nominally parallel to the C_5 rings) is disordered,[22] and the structure has thwarted refinement. Thus, the information gleened from the ordered cation and location and anion planes enables the confident comparison of the ordered MeCN solvate structure to its disordered desolvated form.

The THF grown complex possesses an intrachain Fe–Fe separation of 10.621 (2) Å which is 0.2 Å longer than observed for the desolvated sample. The interchain Fe–Fe separations of 8.020, 8.056, 8.689, 9.618, and 9.649 Å are comparable to the 8.603, 8.732, 9.473, and 9.651 Å observed for MeCN containing phase. Thus, although the intrachain distances are a little longer, a pair of interchain Fe–Fe distances are shorter. In both phases parallel chains are in-registry or out-of-registry (by $b/2$ and $a/2$ for the solvated and desolvated complexes, respectively). Thus, because of the similarity of the strucutres we can obtain a qualitative understanding of the spin interactions within the system by reviewing the in-registry and out-of-registry inter- and intrachain interactions for the MeCN-solvated complex.

The unit cell of $[Fe(C_5Me_5)_2][TCNE]\cdot MeCN$ possesses two pair of chains with interchain separations less than 10.415 Å: an out-of-registry pair separated by 8.232 Å (Chains I–II), Figure 5a, and a pair of in-registry chains (II–III), separated by 8.732 Å, Figure 5b. The nearest neighbor intrachain Fe–N separations range from 5.628–6.471 Å with each $[TCNE]^{\cdot-}$ having average Fe–N distances of 6.016 [±0.34 (6%)]Å and 6.053 [±0.42 (7%)]Å, Figure 5a.

Out-of-Registry Interactions (Chains I–II). Chains I and II are related by inversion symmetry Figure 5a. The interchain Fe–Fe distances are 9.473 and 10.028 Å, whereas several Fe–N separations are less than 10.415 Å, i.e., 5.670–9.943 Å. Two of these four distances (5.670 and 5.707 Å) are comparable with the shorter intrachain Fe–N distances. There are 14 interchain-$[TCNE]^{\cdot-}$ N–N separations less than 10.415 Å; two distances (5.255 and 6.566 Å) are comparable to the intrachain Fe–N separations.

In-Registry Interactions (Chains II–III). Chains II and III are related by a twofold axis with an Fe–Fe separation of 8.732 Å, Figure 5b. All of the interchain Fe–N distances area minimum of 1.9 Å shorter than the intrachain Fe–N distances which range from 8.378–13.479 Å. Consequently, interchain donor/acceptor interactions are not expected to dominate bewteen these chains. A relatively short N–N separation of 4.721 Å is also present.

Chemistry. The preparation of single crystals of $[Fe(C_5Me_5)_2]^{\cdot+}[TCNE]^{\cdot-}$ (as well as $[Co(C_5Me_5)_2]^+[TCNE]^{\cdot-}$)

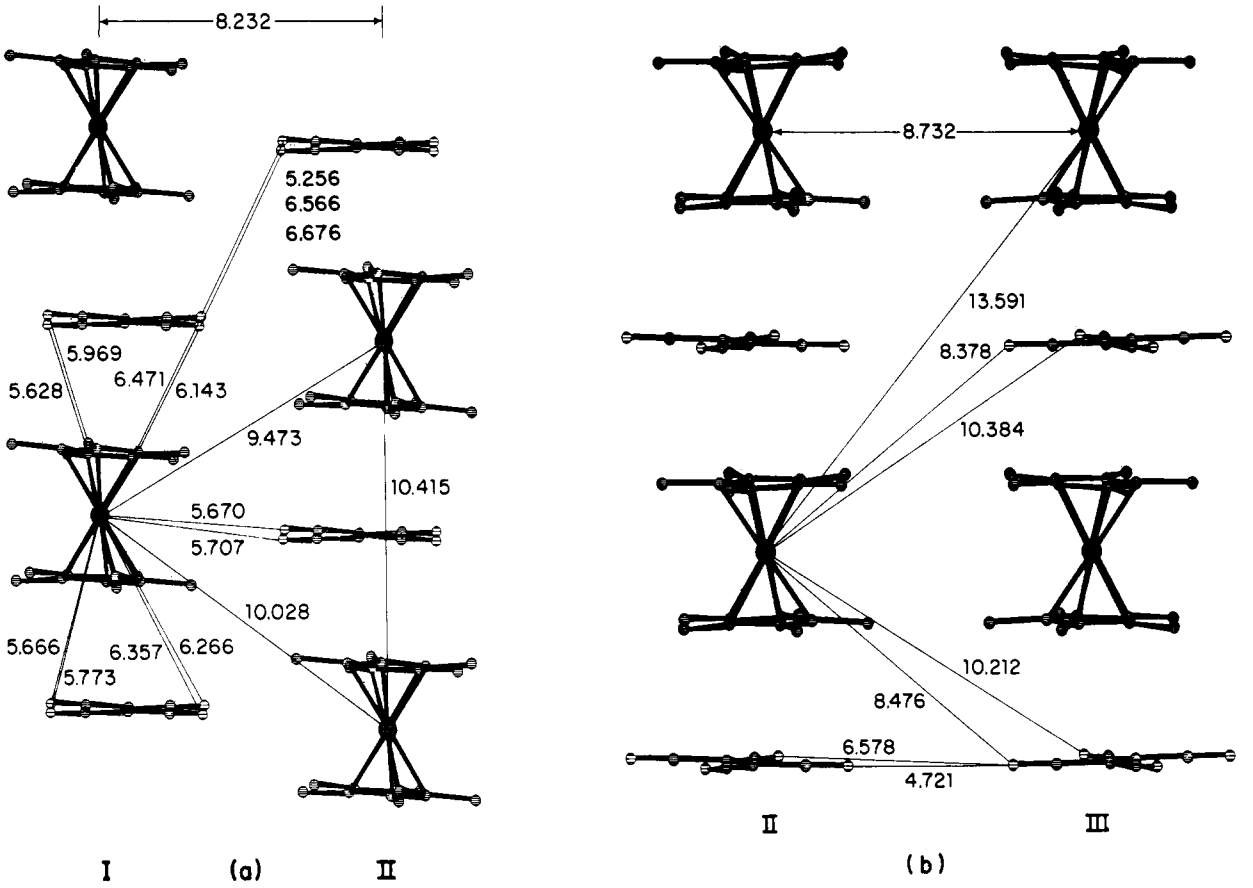

Figure 5. In-registry chains I–II (a) and out-of-registry chains II–III (b) with the intra- and interchain Fe–N, N–N, and Fe–Fe distances.

Table XIV. Metric Parameters for Selected $[Fe(C_5R_5)]^{\bullet+}$ Cations

	local symmetry	Fe–C_5–ring centroid, Å	Fe–C, –Å	C–C, Å	C–Me	C_5–anion, Å	C_5–anion, Å dihedral angle, deg	intrachain Fe–Fe	ref
$Fe(C_5H_5)_2$	D_{5d}	1.656 (4)	2.108 (4)	1.40 (2)					33
$[Fe(C_5H_5)_2]_3[(NC)_2C{=}C(O)CN]_2$	D_{5h}	1.700 (2)[b]	2.073	*a*		3.47	9.3		33
$[Fe(C_5H_5)_2][TCNE]$		1.660	2.037	*a*		3.28		9.9	31, 33
$[Fe(C_5Me_5)_2]^{\bullet+}[TCNE]^{\bullet-}$	D_{5d}	1.70	2.086	1.410	1.499	3.51	2.8	10.415	this work
$[Fe(C_5Me_5)_2]^{\bullet+}[DDQ]^{\bullet-}$		1.712	2.096	1.422	1.505	3.564	3.33	10.616	18a
$[Fe(C_5Me_5)_2]^{\bullet+}[TCNQ]^{\bullet-}$	D_{5d}	1.694	2.096	1.416	1.509	3.67	3.9	10.549	17
$[Fe(C_5Me_5)_2]^{\bullet+}{}_2[TCNQ]_2^{2-}$	D_{5h}		2.090 (7)	1.400 (7)	1.515 (9)	3.554	0	13.997	17
$[Fe(C_5Me_5)_2]^{\bullet+}[C(CN)_3]^-$	C_5	1.710	2.092	1.423	1.498				16
$[Fe(C_5Me_5)_2]^{\bullet+}[C_3(CN)_5]^-$	C_5	1.710	2.095	1.423	1.501	3.44	0	10.35	this work
$[Fe(C_5Me_5)_2]^{\bullet+}[FeCl_4]^-$	C_5		2.090	1.421 (2)	1.495				36
$[Fe(C_5Me_5)_2]^{\bullet+}[FeBr_4]^-$	C_5	1.694	2.092	1.43	1.50				36
$[Fe(C_5Me_5)_2]$	D_{5d}	1.656	2.050	1.419	1.502				32a, 49
$Fe(C_5Me_4H)_2$	C_{2h}	1.656	2.054	1.428	1.496				49
$[Fe(C_5Me_5)_2]^{\bullet+}$ cation ave		1.70	2.09	1.42	1.50				

[a] Disordered. [b] Cation.

Table XV. ^{57}Fe Mössbauer Parameters for $[Fe(C_5Me_5)_2]^{\bullet+}[C_3(CN)_5]^-$

temp, *T*, K	isomer shift,[a] δ, min/s	line width, Γ, min/s
300	0.427	0.323
12.02	0.597	0.865
10.09	0.579	0.914

[a] Relative to natural iron foil.

Table XVI. Internal Hyperfine Fields for $[FeC_5Me_5)_2]^+[TCNE]^-$

T, K	H_{int}, kG
9.00	382.10
8.00	391.20
6.00	426.65
4.23	425.58

suitable for single crystal physical measurements have been problematical. Monoclinic crystals of the acetonitrile solvate readily form; however, solvent is rapidly lost, and the monoclinic lattice transforms into an orthorhombic lattice upon harvesting of the crystals. Elemental analyses of these samples are consistent with the complete loss of MeCN. Large apparent single needle crystals diffract as powders due to the loss of MeCN (vide supra). Single crystals, albeit small, of the orthorhombic phase can be prepared from THF. Ambient recrystallization lead to the isolation of the $[C_3(CN)_5]^-$ salt. The $[C_2(CN)_4]^{\bullet-}$ conversion to $[C_3(CN)_5]^-$ has been reported to occur via reaction of $[TCNE]^{\bullet-}$ with oxygen,[19,27-29,38] Scheme I. Oxidation also forms $[(NC)_2$-

(35) Becker, P.; Coppens, P.; Ross, R. K. *J. Am. Chem. Soc.* **1973**, *95*, 7604–7609.
(36) Zhang, J. H.; Reiff, W. M.; Miller, J. S., manuscript in preparation.

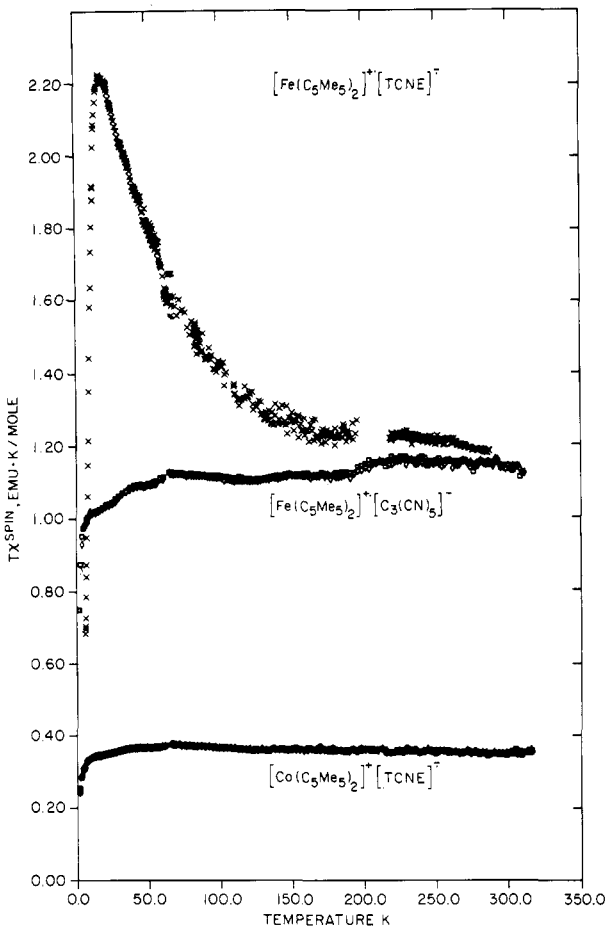

Figure 6. Product of magnetic susceptibility and temperature for $[Fe(C_5Me_5)_2]^{\bullet+}[C_3(CN)_5]^-$ (20.5 kG), $[Co(C_5Me_5)_2]^+[TCNE]^{\bullet-}$ (20.5 kG), and $[Fe(C_5Me_5)_2]^{\bullet+}[TCNE]^{\bullet-}$ (75 kG) as a function of temperature.

Scheme I

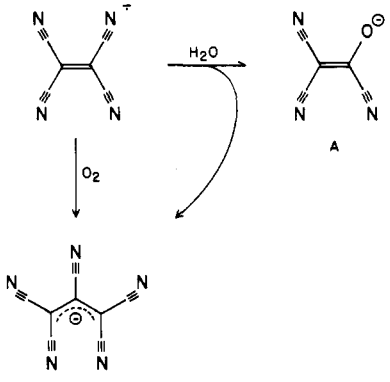

$C{=}C(O)CN]^-$,[19,33] **A**. Likewise, air converts the isolated $[TCNQ]^{\bullet-}$ in the 1-D salt of $[Fe(C_5Me_5)_2]^{\bullet+}$ to the analogous product, i.e. $[p\text{-}(NC)_2CC_6H_4C(O)CN]^-$.[30] Thus, extra precautions to exclude oxygen were taken as the conversion of $[Fe(C_5Me_5)_2][TCNE]$ to the $[C_3(CN)_5]^-$ and $[(NC)_2C{=}C(O)CN]^-$ salts is feasible. For the latter anion the unusual $[Fe(C_5H_5)_2]_3[(NC)_2C{=}C(O)CN]_2$ salt was prepared and characterized by X-ray diffraction[33] and Mossbauer spectroscopy.[39]

Magnetic Susceptibility. $[Co(C_5Me_5)_2]^+[TCNE]^{\bullet-}$ and $[Fe(C_5Me_5)_2]^{\bullet+}[C_3(CN)_5]^-$. Above 2 K the corrected[40] molar magnetic susceptibilities of $[Fe(C_5Me_5)_2]^{\bullet+}[C_3(CN)_5]^-$ and $[Co(C_5Me_5)_2]^+[TCNE]^{\bullet-}$ at 20.5 kG obey the Curie–Weiss expression, i.e., $\chi = C/(T-\theta)$, with small negative values of θ {$\theta = -1.0 \pm 0.3$ K for $[Co(C_5Me_5)_2]^+[TCNE]^{\bullet-}$ and $\theta = -1.2 \pm 0.4$ K for $[Fe(C_5Me_5)_2]^{\bullet+}[C_3(CN)_5]^-$}, Figures 6 and 7. The θ's are characteristic of ferrocenium complexes {e.g., $\theta = -1.33$ and -4.23 for $[Fe(C_5H_5)_2][I_3]$ and $[Fe(C_5H_5)_2]_2[DDQ]_2$,[18b] respectively[41a]} and suggest a small amount of intermolecular antiferromagnetic interaction between the radical cations. Likewise the $[DDQ]^{\bullet-}$ organic radical as the $S = 0$ $[Co(C_5Me_5)_2]^+$ salt possesses a similar θ ($\sim -1 \pm 1$ K).[18b] The effective moment, μ_{eff} [$\equiv 2.83(\chi T)^{1/2}$], varies from 1.72 μ_B for $[Co(C_5Me_5)_2]^+[TCNE]^{\bullet-}$ to 2.99 μ_B for $[Fe(C_5Me_5)_2]^{\bullet+}[C_3(CN)_5]^-$. The lower value is characteristic of $S = {}^1/_2$ radical anions, whereas the 2.99 μ_B value is higher than expected based on previous values ranging from $\sim$2.0 to 2.7 μB[41,42] for ferrocenium salts and suggests that there are alignment effects and significant orbital contributions to the moment over and above the spin only value of 1.73 μ_B. The $g_\parallel$ for $[Fe(C_5Me_5)_2]^{\bullet+}$ has been reported to be $\sim 4.40 \pm 0.03$ (with $g_\perp \sim 1.3$)[41b] and is more anisotropic than that reported for $[Fe(C_5H_5)_2]^{\bullet+}$; thus, the 2.99 μ_B μ_{eff} value is not unexpected for an anisotropically aligned sample. Hence, for ···DADA··· chains where either the D or A but not both is a $S = {}^1/_2$ radical, weak antiferromagnetic behavior is observed.

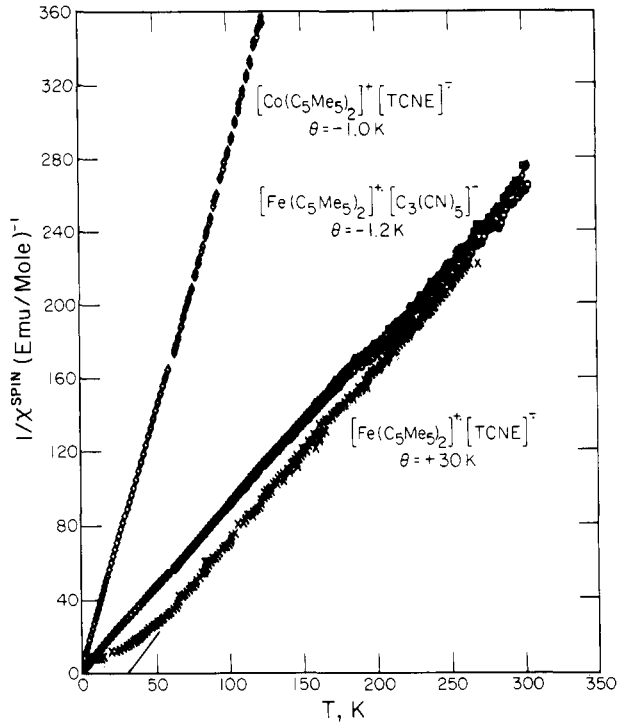

Figure 7. Fit to Curie–Weiss expression of χ_M^{-1} vs. T for $[Fe(C_5Me_5)_2][TCNE]\cdot MeCN$ (75 kG), $[Co(C_5Me_5)_2][TCNE]$ (20.5 kG) and $[Fe(C_5Me_5)_2][C_3(CN)_5]$ (20.5 kG).

$[Fe(C_5Me_5)_2]^{\bullet+}[TCNE]^{\bullet-}$. In contrast to ···DADA··· structures possessing either a $S = {}^1/_2$ D or $S = {}^1/_2$ A, substantial cooperative magnetic interactions may be observed when both the D and A are $S = {}^1/_2$ radicals, i.e., $[Fe(C_5Me_5)_2]^{\bullet+}[TCNE]^{\bullet-}$. The magnetic susceptibility of $[Fe(C_5Me_5)_2]^{\bullet+}[TCNE]^{\bullet-}$ was measured by the Faraday technique between 1.7–300 K and 300–75 000 G. The reciprocal molar spin susceptibility,[40] χ_M^{-1}, at 75 000 G is plotted as a function of temperature, Figure 7. Above 60 K this complex

(37) Reis, A. H., Jr.; Preston, L. D.; Williams, J. M.; Peterson, S. W.; Candela, G. A.; Swartzendruber, L. J.; Miller, J. S. *J. Am. Chem. Soc.* **1979**, *101*, 2756–2757.

(38) (a) Rosenblum, M.; Fish, R. W.; Bennett, C. *J. Am. Chem. Soc.* **1964**, *86*, 5166–5170. (b) Cram, D. J.; Trueblood, T. N. *J. Am. Chem. Soc.* **1959**, *81*, 3971.

(39) Roberts, R. M. G.; Silver, J. *Inorg. Chim. Acta* **1985**, *102*, 51–53.

(40) The diamagnetic corrections of $-230{\cdot}10^{-6}$ emu/mol for $M(C_5Me_5)_2$(M = Co, Fe)[18a], $-57{\cdot}10^{-6}$emu/mol for TCNE (Rosenblum, M.; Fish, R. W.; Bennett, C. *J. Am. Chem. Soc.* **1964**, *86*, 5166–5170), and $-90{\cdot}10^{-6}$emu/mol for $[C_3(CN)_5]^-$ were used.

(41) (a) Morrison, W. H., Jr.; Krugsrud, S.; Hendrickson, D. N. *Inorg. Chem.* **1973**, *12*, 1998–2004. (b) Morrison, W. H., Jr.; Hendrickson, D. N. *Inorg. Chem.*, **1975**, *14*, 2331–2346.

(42) Hendrickson, D. N.; Sohn, Y. S.; Gray, H. B. *Inorg. Chem.* **1971**, *10*, 1559–1563.

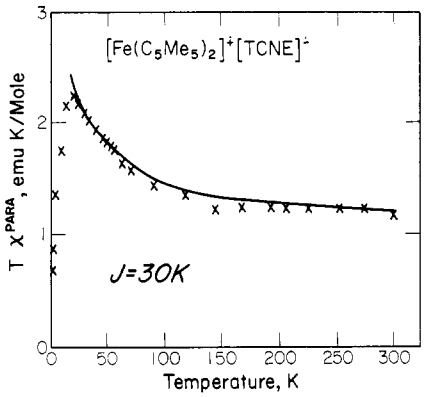

Figure 8. $\chi_M T$ vs. T fit for $[Fe(C_5Me_5)_2][TCNE]$ by the $S = {}^1/_2$ 1-D Heisenberg equation, i.e., eq 1, with ferromagnetic coupling.

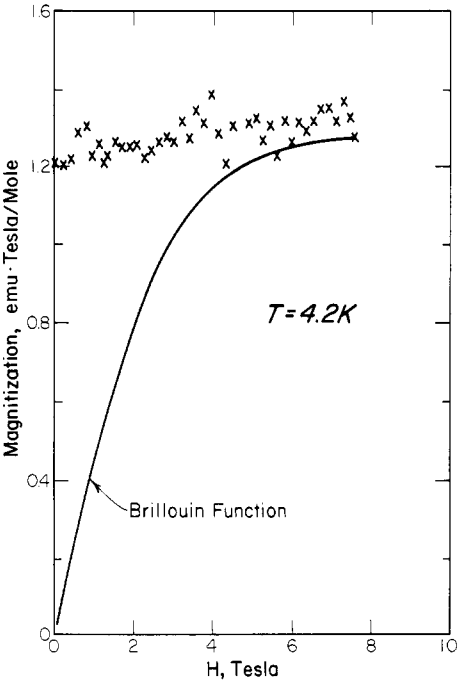

Figure 9. Saturation magnetization as a function of field, M(H), at 4.2 K.

obeys the Curie–Weiss expression, i.e., $\chi = C/(T - \Theta)$, $\Theta = +30$ K (μ_{eff} evaluated at room temperature is 3.10 μ_B), demonstrating that this complex has dominant bulk ferromagnetic interactions. The data plotted as $T\chi$ vs. T are shown in Figure 6. The approach toward saturation of the magnetic moment at 75 kG and $T < 16$ K leads to an apparent decrease in χT at lower temperatures. For temperatures above 16 K (the maximum in Figure 6) preliminary calculations suggest that χ can be fit by a $S = {}^1/_2$ 1-D Heisenberg model with ferromagnetic exchange,[43] Figure 8, as shown in eq 1

$$\frac{\chi(K)}{Ng^2\mu_B{}^2} = \left[\frac{(1 + 5.80\ K + 16.90\ K^2 + 29.38\ K^3 + 29.83\ K^4 + 14.04\ K^5)}{(1 + 2.80\ K + 7.01\ K^2 + 8.65\ K^3 + 4.57\ K^4)}\right]^{2/3} \quad (1)$$

(43) (a) Baker, G. A., Jr.; Rushbrooke, G. S.; Gilbert, H. E. *Phys. Rev.* **1964**, *135*, A1272–A1277. (b) Swank, D. D.; Landee, C. P.; Willett, R. D. *Phys. Rev., B* **1979**, *20*, 2154–2162.

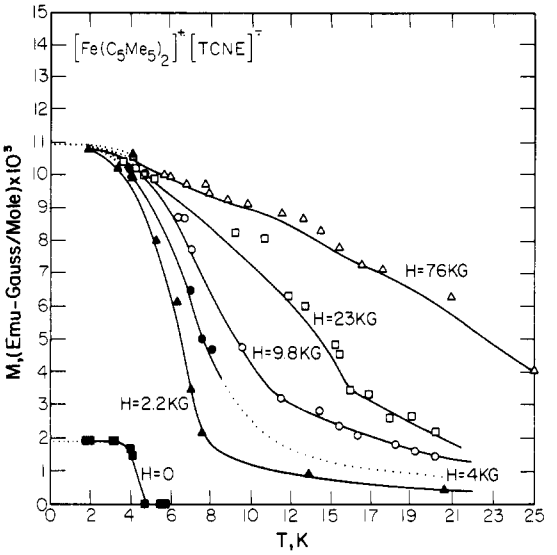

Figure 10. Temperature dependence of the magnetization as a function of applied fields for polycrystalline samples of $[Fe(C_5Me_5)_2][TCNE]$.

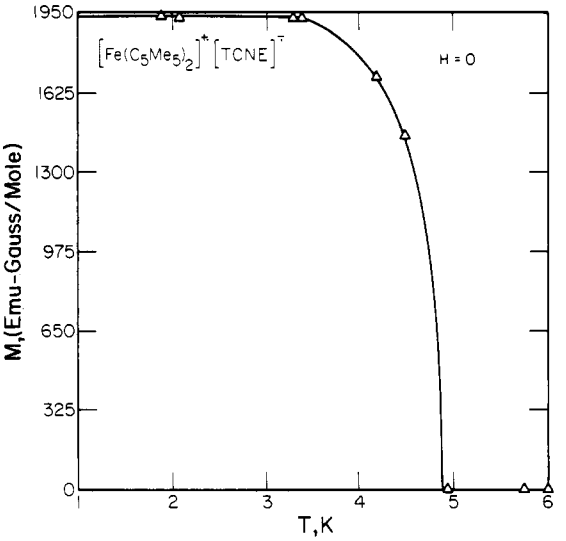

Figure 11. Zero applied field temperature dependence of the magnetization for polycrystalline samples of $[Fe(C_5Me_5)_2][TCNE]$.

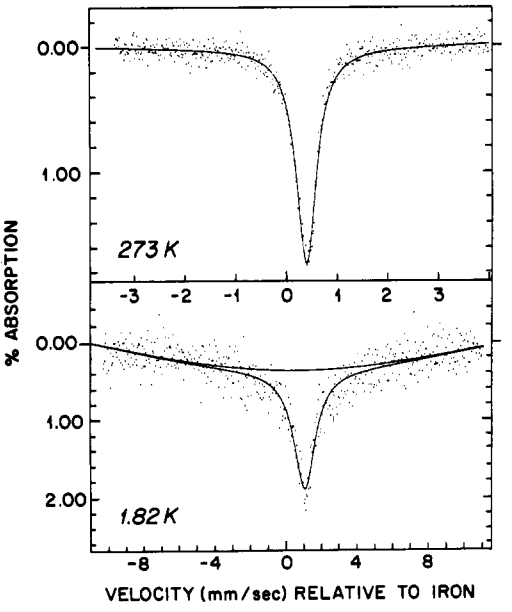

Figure 12. ^{57}Fe Mossbauer spectra at 273 and 1.82 K for $[Fe(C_5Me_5)_2][C_3(CN)_5]$.

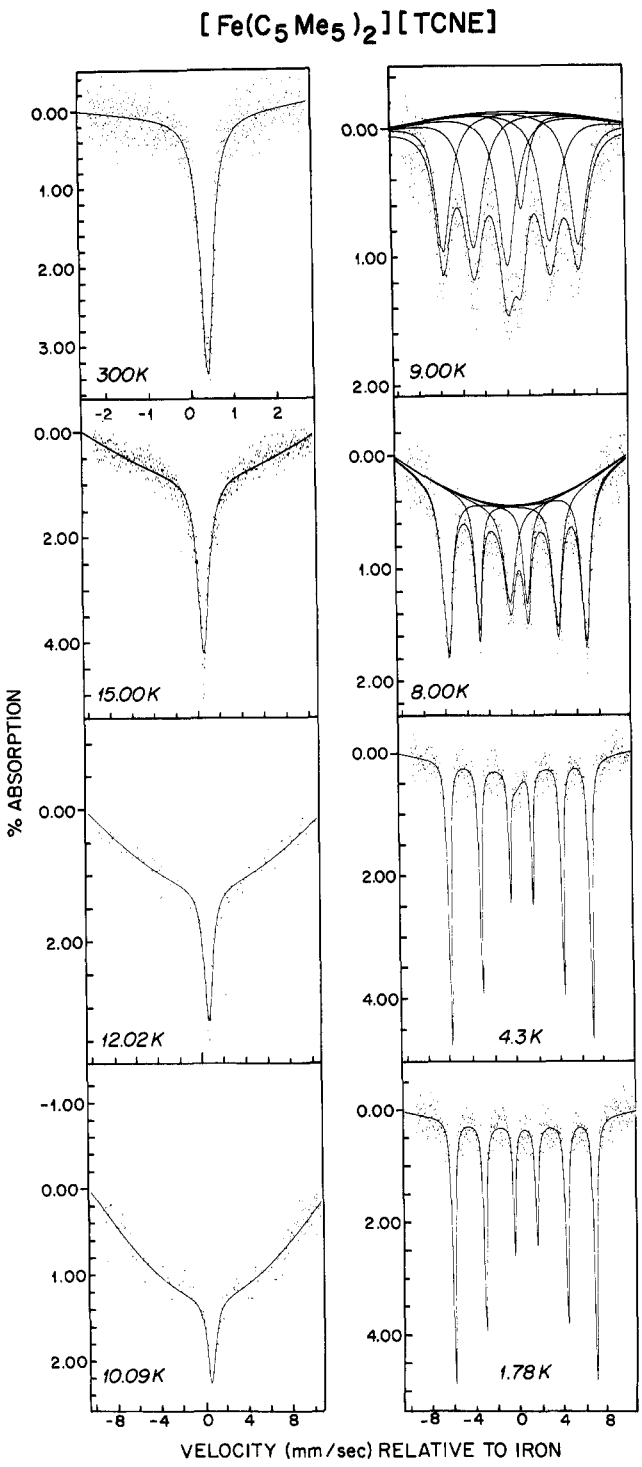

Figure 13. Temperature dependence ($1.78 < T < 300$ K) of the ^{57}Fe Mossbauer spectra of $[Fe(C_5Me_5)_2][TCNE]$.

where $K = J/2k_BT$ and k_B is the Boltzmann constant. The best fit is obtained for $J = 30$ K. Below 16 K 3-D ordering dominates, and the calculated and observed data differ. For the polycrystalline samples the magnetization at 4.23 K saturates to a value of 1.1 ± $0.1 \cdot 10^4$ emu·G/mol for magnetic fields greater that 300 G, Figure 9. Unlike $[Fe(C_5Me_5)_2]^{\bullet+}[TCNQ]^{\bullet-}$ we do not have any evidence for metamagnetism, i.e., $[Fe(C_5Me_5)_2]^{\bullet+}[TCNE]^{\bullet-}$ has a 3-D ferromagnetic ground state at 300 G as opposed to the antiferromagnetic ground state observed for metamagnetic $[Fe(C_5Me_5)_2]^{\bullet+}[TCNQ]^{\bullet-}$.[7]

In zero applied field a spontaneous magnetization is observed for $T < 4.5$ K. Below 4.5 K the magnetization saturates to 1.1 ±$0.1 \cdot 10^4$ emu·G/mol) at progressively lower applied fields, Figure 10. In zero applied field a spontaneous magnetization of ~$2 \cdot 10^3$ emu·G/mol is observed, Figure 11. This decrease in magnetization may be due to orientational effects in the polycrystalline sample, domain formation, or ferrimagnetic behavior. The $\chi_M^{-1}(T)$ data, however, is unlike that of a typical ferrimagnet, i.e., a Neël hyperbola.[44] The shapes of the M(H,T) curves are qualitatively similar for a 3-D ferromagnet.[45] Thus, $[Fe(C_5Me_5)_2][TCNE]$ exhibits spontaneous magnetization in zero applied field consistent with a 3-D (bulk) ferromagnetic ground state.

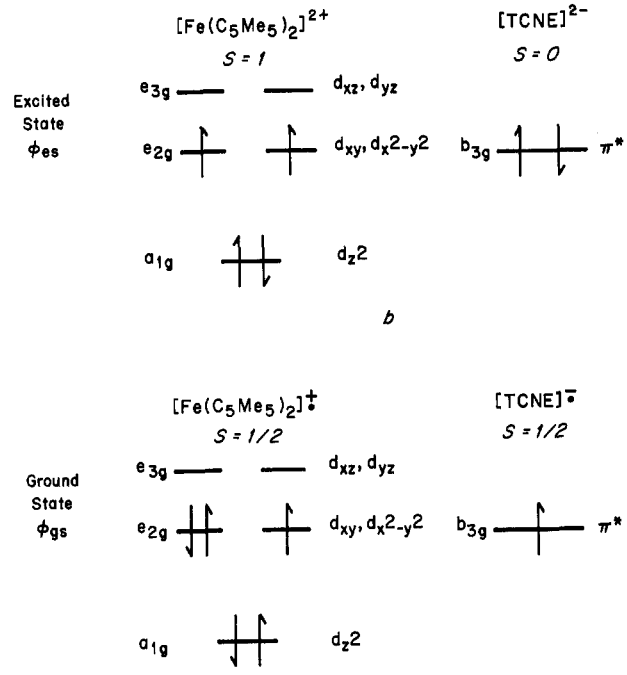

Figure 14. Ground and excited state electronic structures for $[Fe(C_5Me_5)_2]^{\bullet+}[TCNE]^{\bullet-}$.

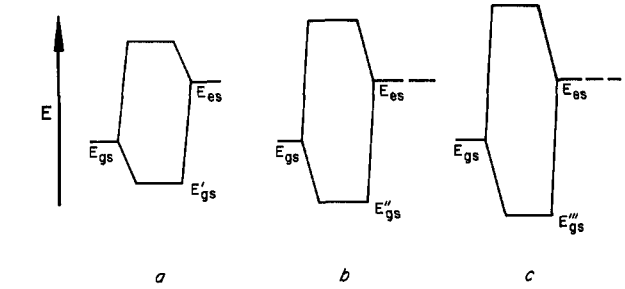

Figure 15. Schematic illustration of (a) mixing of ground state and $S = 1$ excited state; (b) mixing of ground state and pair of intrachain localized excited states; and (c) mixing of ground state and pair of intrachain and interchain localized excited states.

Mossbauer Spectra. At ambient temperature the ^{57}Fe Mossbauer spectrum of $[Fe(C_5Me_5)_2][TCNE]$ and $[Fe(C_5Me_5)_2][C_3(CN)_5]$ exhibit a single transition characterized by a relatively narrow line width (Γ ~0.323 mm/s), i.e., no resolved quadrupole interaction, and an isomer shift relative to natural iron of 0.427 mm/s, Table XV, and Figures 12 and 13. These values are typical of ground spin doublet ferrocenium ions.[47] Singlet spectra are also observed at low temperatures for $[Fe(C_5Me_5)_2]^{\bullet+}$ salts containing diamagnetic anions, e.g., $[C_3(CN)_5]^-$, Figure 12. We have recently found that, in general, below 20 K $[Fe(C_5Me_5)_2]^{\bullet+}[anion]^{\bullet-}$[17,18b,48] systems exhibit resolved magnetic

(44) Helms, J. H.; Hatfield, W. E.; Kwiecien, M. J.; Reiff, W. M. *J. Chem. Phys.* **1986**, *84*, 3993–3998.
(45) Chittipeddi, S. R.; Epstein, A. J.; Reiff, W. M.; Zhang, J. H.; Miller, J. S., unpublished.
(46) Ziman, J. M. *Principles of the Theory of Solids*; 2nd ed.; Cambridge University Press: London, England, 1965; p 290ff.
(47) Wertheim, G. K.; Herber, R. H., Jr. *J. Chem. Phys.* **1963**, *38*, 2106.
(48) Miller, J. S.; Zhang, J. H.; Reiff, W. M., manuscript in preparation.

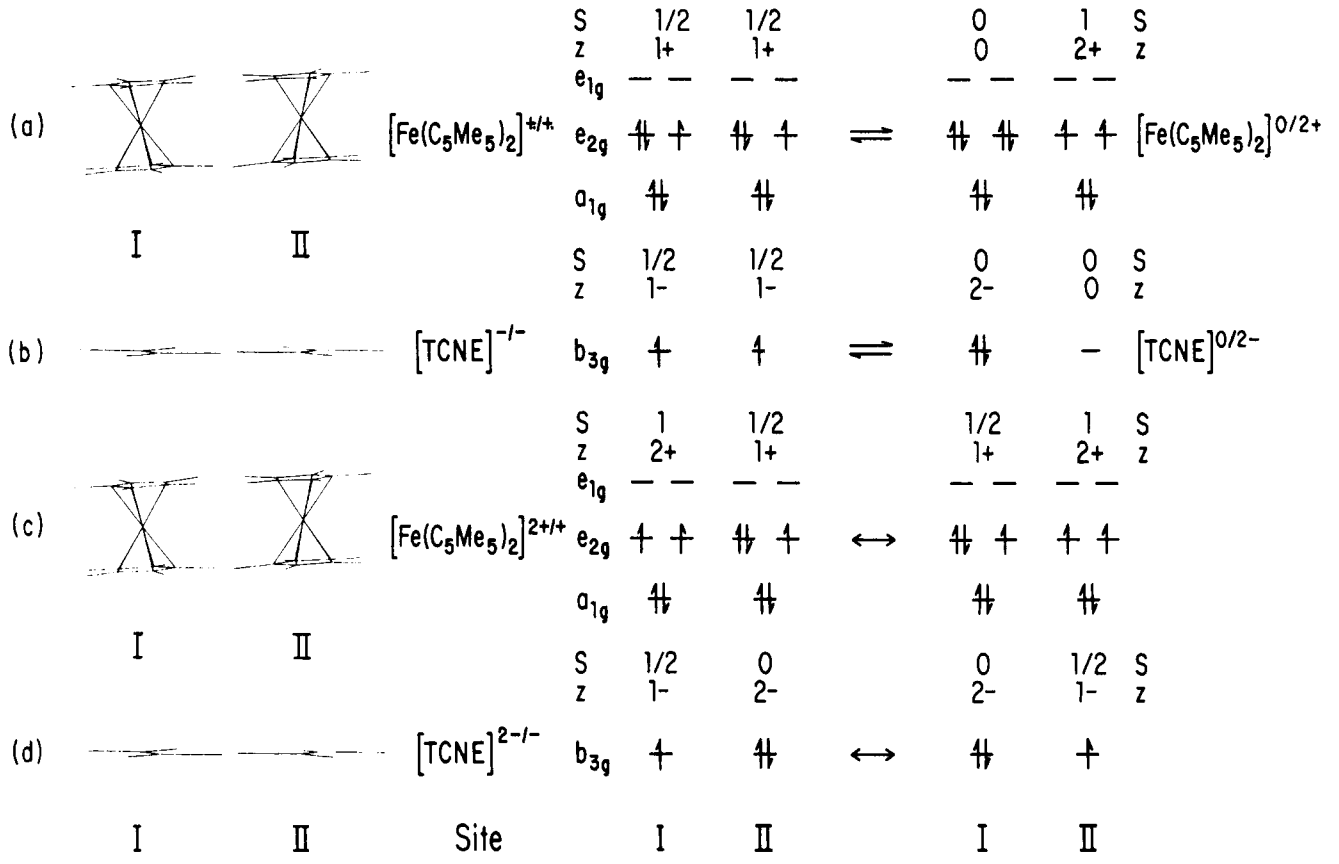

Figure 16. (a) Disproportionation of in-registry $[Fe(C_5Me_5)_2]^{+\bullet}$'s to form $S = 1$ $[Fe(C_5Me_5)_2]^{2+}$ and $S = 0$ $[Fe(C_5Me_5)_2]^0$ which can lead to ferromagnetic exchange.[51a] (b) Disproportionation of adjacent in-registry $S = {}^1/_2$ $[TCNE]^{-\bullet}$'s to form $S = 0$ $[TCNE]^{2-}$ and $S = 0$ $[TCNE]^0$ which can lead to antiferromagnetic exchange.[51b] (c) Cation 2+/+ [(d) and anion 2−/1−] electron transfer (spin exchange) between adjacent in-registry interchain sites I and II.

hyperfine splittings when the anion is paramagnetic. These hyperfine splitting processes correspond to various combinations of slow paramagnetic relaxation broadening and cooperative three-dimensional ordering processes depending on the radical anion. For $[Fe(C_5Me_5)_2]^{+\bullet}[TCNE]^{-\bullet}$ the 4.23 K spectrum in zero applied magnetic field corresponds to a single internal hyperfine field, H_n, of 426 kG, Figure 13. The internal field is temperature dependent and varies from 382.1 (9 K) to 425.6 kG (4.23 K), Table XVI. The latter values of H_n are anomalously large in view of the usual expectation of 110 kG/spin on the iron atom from the Fermi contact H_f contribution and suggests a dominant orbital contribution H_L to H_n. High field Mossbauer spectra experiments bearing on the nature of H_n for these materials are in progress. If an orbital contribution to H_n is dominant, such experients should show $H_n > 0$ as opposed to the usual observation of $H_n < 0$. The hyperfine splitting process for $[Fe(C_5Me_5)_2]^{+\bullet}[TCNE]^{-\bullet}$ initiates at ~12 K and is nearly fully resolved at 10 K. This process is essentially coincident with the inflection point in the 9.8 kG magnetic field susceptibility data and is consistent with cooperative three-dimensional ferromagnetic ordering for which the Curie temperature, T_c, is below 16 K in consideration of both the susceptibility and zero field Mossbauer spectroscopy data. A more precise value for T_c awaits heat capacity measurements. In addition, careful Mossbauer line shape analysis for the spectra taken around T_c should establish whether the line width broadening is due to single ion relaxation or to a cooperative effect involving solitons in a 1-D magnet.[50]

Physical Model for Molecular Ferromagnetism. We have demonstrated that $[Fe(C_5Me_5)_2]^{+\bullet}[TCNE]^{-\bullet}$ ($S_{TOT} = S_D + S_A = 1$) unlike for $S_{TOT} = {}^1/_2$ $[Fe(C_5Me_5)_2]^{+\bullet}[C_3(CN)_5]^-$ and $[Co(C_5Me_5)_2]^+[TCNE]^{-\bullet}$ exhibits dominant ferromagnetic interactions. Thus, the presence of spin on both ground-state ions appear mandatory. McConnell's 1967 model[14] suggests a conceptual framework to begin to understand the microscopic physical origins of ferromagnetic behavior in this class of alternating $S = {}^1/_2$ donor and $S = {}^1/_2$ acceptor charge-transfer compounds. Recalling from the introduction, McConnell stated that if a $S = 1$ excited state arising from either a $S = 1$ donor or $S = 1$ acceptor but not both[15,51a] is available to mix with the ground state upon virtual charge transfer, then ferromagnetic coupling will be stabilized.[14,15] This model does not, however, discuss how bulk ferromagnetism is achieved. Nonetheless, the $[Fe(C_5Me_5)_2]^{+\bullet}$ cation like $[Fe(C_5H_5)_2]^{+\bullet}$ has a $S = {}^1/_2$ $a_{1g}^2e_{2g}^3$ $[(d_z^2)(d_{x^2-y^2})(d_{xy})]$ ground state,[19a,52] Figure 16a, and upon virtual transfer of an e_{2g} electron to the b_{3g} π^* orbital of $[TCNE]^{-\bullet}$ forming $S = 0$

(49) Struchkov, Yu. T.; Andrianov, V. G.; Sal'Nikova, T. N.; Lyatifov, I. R.; Materikova, R. B. *J. Organomet. Chem.* **1978**, *145*, 213–223.

(50) Thiel, R. E.; DeGraaf, H.; DeJongh, L. J. *Phys. Rev. Lett.* **1981**, *47*, 1415.

(51) (a) For an e^3 donor, D (or acceptor, A) − s^1 A (or D) (s = nondegenerate orbital of a or b symmetry) system only electron transfer to form an $S = 1$ e^2–s^2 excited state could stabilize ferromagnetic coupling via mixing with the ground state. An e^3 D (or A) − e^1 A (or D) would stabilize antiferromagnetic exchange as implied by Breslow;[15] however, other combinations of $S = {}^1/_2$ D and A orbitals, e.g., $e^1 - e^1$ (or $e^3 - e^3$) could also stabilize ferromagnetic coupling. In fact D and A with an e^1–e^1 ground state is prefered as unlike our e^3–s^1 system either forward (D→A) or retro (A→D) charge transfer leads to ferromagnetic coupling. Furthermore, the e^1–e^1 combination is not limited to D–A system but conceivably could be achieved in a homomolecular system via virtual disproportionation. We invoke this type of interaction as an additional mechanism for stabilizing ferromagnetic coupling between adjacent in-registry $[Fe(C_5Me_5)_2]^{+\bullet}$'s (vide infra) (Miller, J. S.; Epstein, A. J., submitted for publication). (b) Using the above argument disproportionation of a pair of adjacent in-registry $S = {}^1/_2$ $[TCNE]^{-\bullet}$ ions (i.e., s^1–s^1) into $S = 0$ $[TCNE]^0$ and an excited state geometry[53] of $S = 0$ $[TCNE]^{2-}$ leads to antiferromagnetic exchange, Figure 16b.

(52) Caulette, C.; Green, J. C.; Kelly, M. R.; Powell, P.; Tilborg, J. V.; Robbins, J.; Smart, J. C.; *J. Electron Spectrosc. Relat. Phenom.* **1980**, *19*, 327–353. Evans, S.; Green, M. L. H.; Jewitt, B.; King, G. H.; Orchard, A. F. *J. Chem. Soc.* **1974**, *70*, 356–376. Sohn, Y. S.; Hendrickson, D. N.; Gray, H. B. *J. Am. Chem. Soc.* **1971**, *93*, 3603–3612.

$[TCNE]^{2-}$[53] a $S = 1$ 2+ cation possessing the $a_{1g}^2e_g^2$ electronic configuration results, Figure 14. Mixing of the ground state, ϕ_{gs}, with the excited state, ϕ_{es}, forms a new ground state ϕ'_{gs} of lower energy, E'_{gs}, Figure 15a. Thus, spin alignment lowers the energy of the $[Fe(C_5Me_5)_2]^{\bullet+}[TCNE]^{\bullet-}$ repeat unit. Since the cation is essentially equidistant to a $[TCNE]^{\bullet-}$ above and below it within a chain, a virtual transfer of its e_{2g} electron forming the excited $S = 1$ state to either $[TCNE]^{\bullet-}$ may occur. Thus, two excited-state configurations could mix with the ground state further lowering the energy to E''_{gs}, Figure 15b. This "spin orientation" can establish along a chain leading to stabilization of the system via spin alignment. Even in the limit that the spins in one ···DADA··· chain are aligned, i.e., ferromagnetically coupled, macroscopic ferromagnetism will not occur unless the spins on each chain are aligned. If the spins on adjacent chains are in the opposite sense, then depending on if the spins completely cancels or not, antiferromagnetic or ferrimagnetic behavior should dominate.

Spin alignment between chains may occur if the $[TCNE]^{\bullet-}$ residing in an adjacent chain is equally proximal to the Fe^{III} as it is the intrachain $[TCNE]^{\bullet-}$'s. If the inter- and intrachain $[TCNE]^{\bullet-}$'s are comparably separated from a Fe^{III}site, then an e_{2g} electron may have similar transfer integrals between chains and may be transferred to a b_{3g} $[TCNE]^{\bullet-}$ π^* orbital on an adjacent chain to further stabilize the system, Figure 15c, and align the spins on adjacent chains. This could lead to macroscopic ferromagnetic interactions. The proximity of $[TCNE]^{\bullet-}$ to Fe^{III} between out-of-registry chains, Figure 5a, is comparable to the intrachain separations, Figure 5b, suggesting that virtual electron transfer between chains is viable. The intrachain Fe–N separations range from 5.628–6.471 Å, whereas the comparable Fe–N separations (i.e., 5.670 and 5.707 Å) are present between chains I and II.

An additional mechanism for spin alignment between chains is electron transfer mediated spin exchange between cations and, independently, spin exchange between anions. The disproportionation via excitation from $[Fe(C_5Me_5)_2]^{\bullet+}$ to an adjacent (in-registry) $[Fe(C_5Me_5)_2]^{\bullet+}$ to form $S = 1$ $[Fe(C_5Me_5)_2]^{2+}$ and $S = 0$ $[Fe(C_5Me_5)_2]^0$, Figure 16a, can lead to ferromagnetic exchange.[53] In addition, an electron could be transferred from a $S = {}^1/_2$ $[Fe(C_5Me_5)_2]^{\bullet+}$ on site II to a virtual $S = 1$ $[Fe(C_5Me_5)_2]^{2+}$ on site I (located on an in-registry adjacent chain), such that the $S = {}^1/_2$ 1+ cation was subsequently on site I and the $S = 1$ 2+ cation on site II, Figure 16c. Likewise, electron transfer (spin exchange) could occur for $S = 0$ $[TCNE]^{2-}$, and $S = {}^1/_2$ $[TCNE]^{\bullet-}$ on adjacent chains, Figure 16d, chains I–II, Figure 5a, possesses parallel chains in-registry such that the cations are in close proximity with cations (as well as anions in close proximity to anions). The interchain Fe–Fe distance is 8.732 Å between chains II–III. Chains II–III also have the shortest interchain N–N separation, i.e., 4.721 Å which is greater than 1 Å shorter than the shortest intrachain N–N distances (5.670 and 5.707 Å).

These interchain interactions support the possibility of disproportionation mediated spin alignment as well as $cation^{2+}$/$cation^{\bullet+}$ and $anion^{2-}$/$anion^{\bullet-}$ electron transfer mediated spin exchange to further stabilize the system and align spins on adjacent chains[51b] which are necessary for macroscopic ferromagnetism.

Summary

The area of molecular based ferromagnetic compounds is in its infancy. Our data demonstrate that ferromagnetism is achievable in molecular systems, and we hope that it will also be observed in totally organic systems. Our system, of course, possesses iron; nonetheless, this charge-transfer complex is more akin to an organic compound than an inorganic solid. The iron in our system is low spin Fe^{III} not high spin Fe^{II} or Fe^{III} or iron metal. Unlike highly magnetic inorganic substances the $[Fe(C_5Me_5)_2]$[anion] complexes are soluble and recrystallizable from conventional polar organic solvents and are insoluble or decompose in aqueous solvents. Furthermore, from a chemical reactivity viewpoint ferrocene's are similar to aromatic organic compounds like benzene.[54] Verification and extention of McConnell's model in our systems as well as preparing and characterizing new highly magnetic compounds, particularly with higher transition temperatures, are in progress.

Acknowledgment. W.M.R. and J.H.Z. gratefully acknowledge support from NSF DMR Solid State Chemistry Program Grant No. 8313710. J.S.M. acknowledges the stimulating discussions with Owen Webster, the NMR data taken by R. Farlee, the low-temperature EPR data taken by P. J. Krusic and D. Jones, magnetic susceptibility data taken by S. McLean and D. C. Johnson, and sample preparation by C. Vazquez (Du Pont CR&DD). We thank W. Pennington (Molecular Structures Corporation) and R. R. Whittle (Oneida Research Services) for their assistance in determining the structure of $[Fe(C_5Me_5)_2]$-[TCNE] prepared from THF.

Registry No. $[Fe(C_5Me_5)_2][TCNE]\cdot MeCN$, 105372-44-9; $[Fe(C_5PMe_5)_2][TCNE]$, 105399-77-7; $[Co(C_5Me_5)_2][TCNE]$, 105372-45-0; $[Fe(C_5Me_5)_2][BF_4]$, 100021-51-0; $[Fe(C_5Me_5)_2][C_3(CN)_5]$, 105372-46-1.

Supplementary Material Available: Tables of the observed and calculated structure factors for $[Fe(C_5Me_5)_2]^{\bullet+}[C_3(CN)_5]^-$ and $[Fe(C_5Me_5)_2]^{\bullet+}[TCNE]^{\bullet-}\cdot MeCN$ (10 pages). Ordering information is given on any current masthead page.

(53) The ground state of $S = 0$ $[TCNE]^{2-}$ is D_{2d};[34] however, the $[TCNE]^{\bullet-}$ from which $[TCNE]^{2-}$ would be made is constrained into a D_{2h} structure. Thus, it is possible that the virtually formed D_{2h} $[TCNE]^{2-}$ might be in the $S = 1$ excited state and both the 2+ cation and 2– anion would be $S = 1$. This situation would be at variance with McConnell's model which specifically requires either the donor or acceptor (but not both)[15,51] to be a triplet for ferromagnetic coupling to occur.

(54) Cotton, F. A.; Wilkinson, G. *Advanced Inorganic Chemistry*, 4th ed.; John Wiley: 1980, p 1166.